Research Square

Preprints are preliminary reports that have not undergone peer review.
They should not be considered conclusive, used to inform clinical practice,
or referenced by the media as validated information.

Cation-exchange recovery of scandium-44 for radiopharmaceutical purposes: post-processing of the 44Ti/44Sc generator eluate

Pavel Miroshin

pmiroshin@fmbcfmba.ru

State Research Center Burnasyan Federal Medical Biophysical Center of Federal Medical Biological Agency: FGBU Gosudarstvennyj naucnyj centr Federal'nyj medicinskij biofiziceskij centr imeni A I Burnazana Federal'nogo mediko-biologiceskogo agentstva Rossii https://orcid.org/0009-0000-1120-9991

Anton Larenkov

State Research Center Burnasyan Federal Medical Biophysical Center of Federal Medical Biological Agency: FGBU Gosudarstvennyj naucnyj centr Federal'nyj medicinskij biofiziceskij centr imeni A I Burnazana Federal'nogo mediko-biologiceskogo agentstva Rossii

Research Article

Keywords: scandium-44, 44Ti/44Sc radionuclide generator, cation exchange, distribution coefficient, oxalate, carboxylate buffer, [44Sc]Sc-PSMA-617, [44Sc]Sc-DOTA-TATE, [44Sc]Sc-FAP-2286

Posted Date: November 17th, 2026

DOI: https://doi.org/10.21203/rs.3.rs-11537752/v1

License: This work is licensed under a Creative Commons Attribution 4.0 International License.
Read Full License

Title page

Cation-exchange recovery of scandium-44 for radiopharmaceutical purposes: post-processing of the $^{44}Ti/^{44}Sc$ generator eluate

Authors: Pavel Miroshin* (https://orcid.org/0009-0000-1120-9991), Anton Larenkov (https://orcid.org/0000-0003-4810-4346)

State Research Center–Burnasyan Federal Medical Biophysical Center of Federal Medical Biological Agency, 123182 Moscow, Russia

*Corresponding author: P.A. Miroshin, e-mail: pmiroshin@fmbcfmba.ru

Word count (main text): ≈ 9200. Figures: 13. Tables: 8. Supplementary Information files: 1.

Abstract

Background. Scandium radionuclides (^{43}Sc, ^{44}Sc, and ^{47}Sc), owing to their favorable decay characteristics and coordination chemistry, attract attention in molecular imaging and targeted therapy, matching with clinically established ^{177}Lu and ^{90}Y, and forming element-matched theranostic pairs. However, clinical translation of accelerator-produced Sc radioisotopes or ^{44}Sc eluted from $^{44}Ti/^{44}Sc$ generators requires a final concentration and conditioning step to deliver Sc(III) in a minimal volume of biocompatible buffer for direct radiolabeling. In this study, nine commercial resins and six carboxylate buffers (30 conditions) were evaluated for single-step Sc(III) recovery enabling direct DOTA-conjugate labeling, using TEVA-based $^{44}Ti/^{44}Sc$ generator eluate (0.1 M $H_2C_2O_4$ / 0.2 M HCl) containing the competing ligand oxalate, and 0.1 M HCl as a model medium.

Results. Static distribution coefficients (D_g) and dynamic column profiles revealed that low-capacity silica-based cation-exchange resins were superior to high-capacity polymeric gels because high-yield desorption into 1 mL required a high eluent Na^+ / capacity ratio. Chromafix HR-XC sorbed 98.4 ± 1.1 % of ^{44}Sc after fivefold generator eluate dilution with water; only Chromabond PSA sorbed ^{44}Sc quantitatively directly from the undiluted eluate (99.0 ± 0.5 %). Across six pharmaceutically acceptable carboxylates (0.2–1.0 M, pH 4.00 ± 0.15), desorption and subsequent DOTA-labeling yields responded oppositely to a single thermodynamic variable: conditional availability of auxiliary Sc–carboxylate complexes, $\log(K_1 \cdot [L])$ (Spearman $\rho = -0.83$). Among 30 conditions, 1 M sodium acetate was the global optimum ($Y_{comb} = Y_{des} \times RCY$: 78.8 ± 1.7 % vs. 72.1 ± 3.3 % for 0.4 M succinate; $p = 0.007$). Acetate elution (1 mL) recovered 80.4 ± 2.7 % (Chromabond PSA) and 79.4 ± 1.7 % (Chromafix HR-XC). Residual oxalate was $<1.6 \times 10^{-3}$ M. The conditioned solution enabled

synthesis of [^{44}Sc]Sc-PSMA-617, [^{44}Sc]Sc-DOTA-TATE and [^{44}Sc]Sc-FAP-2286 (RCY 96.6–98.2 %; 0.63–0.96 nmol precursor; apparent molar activities up to 50.0 ± 1.2 MBq/nmol).

Conclusions. Two rapid (11–15 min) conditioning schemes provided ^{44}Sc for direct labeling at 4–5-fold higher volumetric activity than extraction chromatography. Established stoichiometric bed-capacity requirements, oxalate tolerance bounds and conditional auxiliary-ligand stability criteria may be transferable to the formulation and radiolabeling of ^{43}Sc, ^{44}Sc, and ^{47}Sc radiopharmaceuticals.

Key words: scandium-44; ^{44}Ti/^{44}Sc radionuclide generator; cation exchange; distribution coefficient; oxalate; carboxylate buffer; [^{44}Sc]Sc-PSMA-617; [^{44}Sc]Sc-DOTA-TATE; [^{44}Sc]Sc-FAP-2286

Background

Scandium radioisotopes (^{43}Sc, ^{44}Sc, and ^{47}Sc) currently attract considerable attention for nuclear medicine applications; however, their widespread use is constrained by the lack of efficient, scalable production methods. ^{44}Sc ($T_{½}$ = 3.97 h, β^+ — 94.3 %, $E\beta^{max}$ = 1474.3 keV) [1] offers decay properties well suited to PET imaging. It has lower mean positron energy (632 keV) than the routinely used ^{68}Ga ($T_{½}$ = 67.83 min, β^+ — 88.9 %, $E\beta^{max}$ = 1899.1 keV) [1], which translates into improved intrinsic spatial resolution, and its longer half-life widens the temporal window for imaging slowly accumulating targeting molecules (up to 24 h) [2,3].

However, ^{44}Sc decay is accompanied by a high-energy prompt γ-ray (Eγ ≈ 1157 keV, ≈ 99.9 %), which increases the dose burden to staff and patients and can degrade image quality. For this reason, ^{43}Sc ($T_{½}$ = 3.89 h, β^+ — > 88 %, $E\beta^{max}$ = 1199 keV) [1] has also attracted attention: it combines a favorable mean positron energy (476 keV) with a lower-energy, lower-intensity γ-ray (Eγ ≈ 372 keV, ≈ 23 %). Production of ^{43}Sc, however, is restricted to accelerators (e.g., ^{43}Ca(p,n)^{43}Sc, ^{42}Ca(d,n)^{43}Sc [4]), whereas ^{44}Sc is available from a ^{44}Ti/^{44}Sc generator. A comparative dosimetry study has shown that the absorbed doses for [^{43}Sc]Sc-DOTA-TATE and [^{44}Sc]Sc-DOTA-TATE exceed those for [^{68}Ga]Ga-DOTA-TATE but remain within clinically acceptable limits [5].

Scandium also offers the therapeutic isotope ^{47}Sc ($T_{½}$ = 3.34 d, β^- = 100 %, Eβ = 162 keV) [1], a soft beta emitter that delivers the dose locally to tumor deposits while sparing surrounding tissue. Its 159 keV γ-ray additionally allows SPECT imaging, dosimetry, and biodistribution monitoring during therapy [6]. The chemical similarity of Sc(III) to yttrium and lanthanides enables the use of the diagnostic isotopes ^{43}Sc and ^{44}Sc in theranostic pairs with ^{177}Lu and ^{90}Y, and with ^{47}Sc to form the matched pairs ^{43}Sc/^{47}Sc and ^{44}Sc/^{47}Sc [7]. Access to scandium radionuclides therefore extends the theranostic approach from diagnosis to dosimetry-guided treatment planning and monitoring.

Scandium radioisotopes are typically produced on medical cyclotrons (proton energy up to 20 MeV) with highly enriched targets (83–98 %) via ^{46}Ti(p,α)^{43}Sc, ^{44}Ca(p,n)^{44}Sc, ^{47}Ti(p,α)^{44}Sc, and ^{50}Ti(p,α)^{47}Sc [8], giving clinically relevant activities: ≈ 200 MBq of ^{43}Sc (> 98 %) [9], > 50 MBq of ^{47}Sc (91.5 ± 0.6 %, the proton beam energy was 24 MeV) [10], and 4.28 GBq of ^{44}Sc (≈ 98 %) [11]. Long-lived scandium impurities nevertheless persist: ^{46}Ti(p,2p)^{47}Sc co-produces ^{46}Sc ($T_{½}$ = 83.8 d) and ^{48}Sc ($T_{½}$ = 1.82 d), and ^{44}Ca(p,n)^{44}Sc co-produces ^{44m}Sc ($T_{½}$ = 58.61 h) [12]. Beyond radionuclidic purity, cyclotron production is limited by infrastructure, as not every clinical center has a cyclotron and an associated radiochemistry facility. A ^{44}Ti/^{44}Sc generator (^{45}Sc(p,2n)^{44}Ti→^{44}Sc) [13,14] offers an alternative: on-site preparation, no transport losses, and installation requirements comparable to those of routine ^{68}Ge/^{68}Ga generators [15].

Purification and concentration are indispensable steps in any scandium production route; extraction chromatography, ion exchange, and chelating resins are used for this purpose (Supplementary Information: Table S1). In the cyclotron production, the purification step also recovers costly enriched target material.

Extraction resins, such as UTEVA and DGA (n-DGA, b-DGA), recover scandium radionuclides from strongly acidic media in which irradiated targets are dissolved, with yields of 79–93 % [10,16–20]. The resulting products are obtained in 0.1 M HCl or, for UTEVA, in ≈ 1 M HCl, and in volumes of 4–5 mL, which limits the attainable activity concentration.

Cation-exchange resins are also employed for the purification of scandium radioisotopes, enabling recovery from weakly acidic media (e.g., 0.1 M HCl) and subsequent elution with a buffer solution suitable for direct use in radiopharmaceutical synthesis. Sc(III) is strongly retained on cation-exchange resins; therefore, desorption requires a complexing agent; acetate buffers are used most often [21,22], and ammonium α-hydroxyisobutyrate (pH 4.8) has been proposed more recently, giving 95 ± 3 % recovery of ^{44}Sc [23]. Bartoś et al. [24] used an anion/cation-exchange scheme (Dowex 1×8 and Dowex 50W×4) to purify ^{47}Sc, obtaining > 90 % in 3 mL of 0.25 M ammonium acetate (pH 4.0); the buffer is compatible with synthesis, but the volume was large. Cingoranelli et al. [25] combined AG MP-50 and CM resins and obtained ^{47}Sc of high radionuclidic purity (99.5 ± 0.2 %) in 1 mL of 2 M HCl, but with a moderate yield (68 ± 4 %) and in a medium unsuitable for direct labelling. Cation-exchange resins thus allow the activity to be concentrated in a smaller volume than solid-phase extractants; therefore, combinations of sorbents are used [11,23,26,27]. Van der Meulen et al. [11,28] and Domnanich et al. [27] combined n-DGA with Bond Elut SCX and obtained the product in 700 µL of ≈ 4.8 M NaCl/0.1 M HCl at > 93 % efficiency; the resulting solution has a calculated osmolality of ≈ 9.9 osmol/kg, which precludes direct administration. Chelating resins, such as Chelex 100, have also been used [20,29], but require either dilute HCl, which gives low recovery, or a large volume of concentrated acid (10 mL of 1 M HNO3, ^{47}Sc yield 95 ± 0.87 %).

Cation-exchange resins and extraction resins are used for the conversion and conditioning of ^{44}Ti/^{44}Sc radionuclide generators. For the AG 1 × 8-based generator (eluted with 0.005 M $H_2C_2O_4$/0.07 M HCl) [30], AG 50W×8 was used to remove oxalate [31], since oxalic acid in the reaction mixture suppresses complexation of ^{44}Sc by the DOTA chelator. For the SnO_2-based generator (eluted with 5 M HNO_3), n-DGA was used to transfer ^{44}Sc into 0.1 M HCl and to remove the parent ^{44}Ti, this generator showing a comparatively high ^{44}Ti breakthrough of 0.14–0.71 % [32].

In the present study, conditioning procedures (post-elution processing**)** were developed for the TEVA-based (Aliquat® 336) ^{44}Ti/^{44}Sc generator [33]. This generator gave a ^{44}Sc elution yield of 91 ± 6 %

with a ^{44}Ti breakthrough of 6.6×10^{-6} % and was operated for more than 120 elutions over one year [33]; the oxalic acid in its eluent (0.1 M $H_2C_2O_4$/0.2 M HCl) nevertheless required post-elution processing. Nine commercially available cation-exchange resins were compared here under identical conditions in batch and in column modes, and six carboxylate eluents were evaluated at five concentrations each.

A cation-exchange conditioning step for this generator has been previously described [34], in which a single resin (Chromafix HR-XC) was used, and the preparation of [^{44}Sc]Sc-PSMA-617 and [^{44}Sc]Sc-DOTA-TATE was reported. The present work provided a systematic comparison of the cation-exchange recovery of ^{44}Sc across nine commercially available cation-exchange resins, evaluated under identical batch and column conditions, including distribution coefficients measured in the actual generator eluate. Quantitative retention of ^{44}Sc directly from the undiluted eluate was achieved on Chromabond PSA at an oxalate concentration twentyfold above the value reported by Pruszyński et al. [31] (0.1 M vs. 0.005 M). Six carboxylate eluents were examined at five concentrations each, and the desorption buffer was selected by an explicit combined criterion rather than by desorption recovery alone. The residual oxalate content was determined analytically by HPLC, and the oxalate concentration in the resulting ^{44}Sc solutions was below the limit of quantification.

This degree of oxalate removal enabled the ^{44}Sc solutions to be successfully applied to the synthesis of three radiotracers: [^{44}Sc]Sc-DOTA-TATE, [^{44}Sc]Sc-PSMA-617, and [^{44}Sc]Sc-FAP-2286. DOTA-TATE is a reference somatostatin analog for PET imaging of neuroendocrine tumors [35], and PSMA-617 is a well-established ligand for prostate cancer imaging and therapy [36]; both served as reference standards for assessing ^{44}Sc solution quality. FAP-2286, a recently introduced ligand targeting fibroblast activation protein (FAP) expressed in the stroma of many epithelial tumors [37,38], was synthesized with ^{44}Sc for the first time in this study.

Methods

Reagents and resins

All procedures used ultrapure water (18.2 MΩ·cm, Milli-Q, Merck Millipore, Darmstadt, Germany) and high-purity or pharmaceutical-grade reagents (PanReac Química, Barcelona, Spain; neoFroxx GmbH, Einhausen, Germany). Cation-exchange resins, given with the abbreviated names used hereafter: Chromabond PSA (propylsulfonic acid on silica) and Chromafix HR-XC (benzenesulfonic acid on styrene–divinylbenzene), Macherey-Nagel, Düren, Germany; AG MP-50 (sulfonic acid, macroporous styrene–divinylbenzene), Bio-Rad, Hercules, CA, USA; Bond Elut SCX (benzenesulfonic acid on silica), Agilent, Santa Clara, CA, USA; Strata-X-C and Strata-X-CW (33 µm; sulfonic and carboxylic acid polymers), Phenomenex, Torrance, CA, USA; OASIS MCX CC (sulfonated divinylbenzene/N-vinylpyrrolidone) and Sep-Pak Accell Plus CM (37–55 µm, carboxymethyl), Waters, Milford, MA, USA; Chromalite CGC 50×2 (sulfonated polystyrene gel), Purolite, Llantrisant, Wales, UK. Key physical characteristics of the resins (matrix, particle size, and nominal exchange capacity) are compiled in Supplementary Information: Table S2. DOTA-TATE (Cat. No.: HY-106244, purity 99.94 %) and FAP-2286 (Cat. No.: HY-147057, purity 99.89 %) were purchased from MedChemExpress (Monmouth Junction, NJ, USA). PSMA-617 (purity ≥ 98.0 %) was kindly provided by LLC "Jenguro" (Moscow, Russia).

Scandium-44

Scandium-44 was obtained from a TEVA-based ^{44}Ti/^{44}Sc generator [33] (new prototype, with nominal ^{44}Ti loading of 50 MBq); ^{44}Ti activity measured at the time of the experiments was 49.2 ± 2.46 MBq; eluent was 1 mL of 0.1 M $H_2C_2O_4$/0.2 M HCl, with a ^{44}Sc yield of 95.6 ± 2.1 % (decay-corrected; mean ± SD, n = 5) and a ^{44}Ti breakthrough of 4.1×10^{-7} %. To exclude any influence of organic species on radiolabelling, a separate series used ^{44}Sc in 0.1 M HCl obtained by oxidative destruction of oxalate: 1 mL of eluate was evaporated to dryness twice with 500 µL of 30 % H_2O_2; the residue was taken up in 70 µL of 1 M HCl and diluted with water to 700 µL. The recovery of ^{44}Sc was 87 ± 3 % (decay-corrected; mean ± SD, n = 5).

Measurement of radioactivity

The activity of ^{44}Sc was measured using an Isomed 2010 dose calibrator (ionization chamber; PTW-Freiburg, Dresden, Germany) with the ^{18}F setting, 2 mL syringe geometry and 1 mL sample volume. Readings were converted to ^{44}Sc activity with a factor of 0.569 (n ≥ 5, activity range 20–45 MBq, relative combined uncertainty ± 5 %), obtained by comparison with absolute activities determined by γ-spectrometry on a GR4020 HPGe spectrometer (Mirion Technologies (Canberra), San Ramon, CA, USA) at 511 and 1157.02 keV (corrected for 511/1157 keV cascade summing). Relative activities (count rates) were measured on a Wizard^2 2480 γ-counter (PerkinElmer, Waltham, MA, USA); count

rates were recorded within the linear range of the detector, after decay of the samples, and were corrected for background and dead time. Radio-TLC strips were scanned on a PET-MiniGita scanner (Elysia-Raytest, Straubenhardt, Germany).

Measurements of ^{44}Ti activity were carried out using an ultra-shielded γ-ray spectrometer equipped with a high-purity germanium (HPGe) detector (GC10021 (Mirion Technologies) with a relative efficiency of 106.8 % (^{60}Co), FWHM 1.02 keV (^{57}Co), and 2.03 keV (^{60}Co) with a DSA-1000 multichannel analyzer and Genie-2000 software (V3.2.1)), at the Laboratory of Radiometric and Spectroscopic Research (Burnasyan Federal Medical Biophysical Center). The measurements were performed at the characteristic γ-lines of 67.9 and 78.3 keV (with control at 1157.02 keV) by a method described previously [33]. The counting time was at least 86400 s, and the minimum detectable activity, calculated by the Currie criterion, was 14×10^{-3} Bq per sample, i.e., 4.5×10^{-8} % of the ^{44}Sc activity of a 31 MBq product.

The contribution of the weighing uncertainty u(m) to the distribution coefficients is included in the reported standard deviations.

Determination of distribution coefficients

The mass distribution coefficient D_g was determined using the batch method [39]. Aliquots of 1 mL of ^{44}Sc solution (0.7–1 MBq) in HCl or $H_2C_2O_4$/HCl of the required concentration, in the undiluted generator eluate or in sodium acetate, were equilibrated with 15.0 ± 0.5 mg of resin (mean ± SD, n = 5). The resins were used as supplied, without preconditioning. Samples were shaken in a temperature-controlled Bioer mixing block (MB-102) (Bioer, Hangzhou, China) for 24 h at 20 °C and 1350 rpm, then centrifuged (Heidolph, Schwabach, Germany) for 1 min at 15,000 rpm. Aliquots of the liquid phase (100–500 μL) were withdrawn without disturbing the resin and counted. D_g (mL/g) was calculated using Eq. (1):

$$D_g = [(A_0 - A)/A] \times (V/m) \qquad (1)$$

where A_0 and A are the count rates of the solution aliquot before and after contact with the resin, respectively, both corrected for decay to a common reference time (s^{-1}); V is the solution volume (mL), and m is the mass of dry resin (g); in SI units, D_g is expressed in $m^3 \cdot kg^{-1}$ (1 mL/g = 1.0×10^{-3} $m^3 \cdot kg^{-1}$). Each D_g was determined in at least five replicates (mean ± SD, n ≥ 5).

The upper limit of quantification of D_g follows from the smallest residual fraction of activity that can be measured reliably ($f_{min} = (A/A_0)_{min}$), and was calculated according to Eq. (2):

$$D_g, \max = (V/m) \cdot (1/f_{min} - 1) \qquad (2)$$

For V/m = 66.7 mL/g and $f_{min} = 1 \times 10^{-2}$, D_g max = 6.6×10^3 mL/g. Values above this limit are reported as censored and are identified as such in Figs. 1 and 2.

Dynamic Column Separation Experiments

Column experiments were performed with PEEK columns of 50 mm × Ø2.1 mm and 100 mm × Ø2.1 mm (VICI Jour, Schenkon, Switzerland). In all cases, the weighed resin completely filled the column volume, and the mass used for each resin is listed in Table 4. Solutions were transferred manually or with a syringe pump using medical-grade syringes (B. Braun Injekt) at 1 mL/min at 20 ± 2 °C. The columns were washed with 1 mL of 95 % ethanol to displace the loading solution and were then dried in a stream of air. ^{44}Sc was desorbed with 1 mL of a sodium carboxylate solution (0.2–1 M; pH 4.00 ± 0.15, adjusted with HCl); sodium acetate was used routinely, and sodium lactate, succinate, pyruvate, α-hydroxyisobutyrate, and malate were examined in a separate series. All percentages reported for column experiments refer to the activity applied to the column. The pH of the eluates was measured immediately after collection.

Separation efficiency under dynamic conditions was evaluated via a ^{44}Sc activity balance. All fractions (post-sorption, wash, and eluate) were measured in a single channel and geometry on the dose calibrator. The column itself was measured in the same channel but in a different geometry. These measurements were used to account for activity losses on the column and assess the effectiveness of the conditioning procedure.

The desorption recovery of Chromafix HR-XC in 1 M sodium acetate was determined twice, in two independent campaigns: in the resin-comparison series (Fig. 7) and in the carboxylate-eluent series (Fig. 10). Both determinations are reported. Values entering the combined criterion Y_{comb} are taken exclusively from the carboxylate-eluent series, so that both factors of the product originate in the same campaign.

Radiolabeling of PSMA-617, DOTA-TATE and FAP-2286

[^{44}Sc]Sc-PSMA-617, [^{44}Sc]Sc-DOTA-TATE, and [^{44}Sc]Sc-FAP-2286 were prepared in a temperature-controlled Bioer mixing block (Bioer MB-102) at 95 °C for 5–30 min at pH 4.00 ± 0.15 in 1.5 mL Eppendorf tubes. The reaction mixture consisted of 980–1000 µL of ^{44}Sc solution (25–33 MBq as delivered by the conditioning step, before decay correction in 0.2–1 M sodium carboxylate, pH 4.00 ± 0.15; usually sodium acetate) and the required amount of precursor (0.63–13.9 nmol, added as 1–20 µL (V_p) of a 1 mg/mL solution), giving a final volume of 1 mL. For the comparison of buffer systems, ^{44}Sc in 0.1 M HCl was used deliberately to separate the effect of the buffer from that of the eluate matrix: 600 µL of ^{44}Sc solution (20–25 MBq), 350 µL of 0.5–3 M buffer, the required amount of precursor (0.63–13.9 nmol, added as 1–20 µL (V_p) of a 1 mg/mL solution), 3 M HCl to adjust the pH to 4.00 ± 0.15, and water to 1 mL, with a final buffer concentration of 0.2–1 M. After synthesis, the pH of each sample was measured using a pH meter.

Two distinct sets of labelling experiments were performed. The kinetic comparison of the four selected resins (Fig. 9) was performed at V_p = 5 µL (4.78 nmol of PSMA-617). The syntheses summarized in Table 6 were performed separately, at V_p = 1 µL for each of the three conjugates (0.96, 0.70, and 0.63 nmol), with n = 5 preparations per product; the yields and activities in Table 6 belong to that series and are not taken from Fig. 9.

Radiochemical yield (*RCY*) is defined here as the fraction of the ^{44}Sc activity introduced into the reaction that is incorporated into the target complex, and radiochemical purity (*RCP*) as the fraction of the activity of the product present as the target complex, in accordance with the consensus nomenclature [40]. Both were determined by radio-TLC in three systems: (i) ITLC-SG (Agilent), 0.05 M citric acid; R_f 0.8–1.0 for [^{44}Sc]Sc^{3+} and 0.1–0.2 for the complexes; (ii) silica gel on aluminum (5553, Merck), acetonitrile–water 1:1; R_f 0.0–0.1 for [^{44}Sc]Sc^{3+}, 0.3–0.5 for [^{44}Sc]Sc-DOTA-TATE and 0.8–1.0 for [^{44}Sc]Sc-PSMA-617 and [^{44}Sc]Sc-FAP-2286; (iii) ITLC-SG, 0.5 M CH_3COONH_4 in methanol–water 1:1; R_f 0.0–0.1 for [^{44}Sc]Sc^{3+} and 0.5–0.6 for the complexes. All radiolabeling yields are reported from system (i), used as the primary system, with systems (ii) and (iii) as confirmatory.

Determination of apparent molar activity

After labelling, the activity of the product was measured in the dose calibrator under the conditions described above, and *RCY* was determined by radio-TLC. The apparent molar activity A_m was calculated using Eq. (3):

$$A_m = (A \times RCY)/n \quad (3)$$

where A is the activity of the product measured with the dose calibrator and corrected as described, decay-corrected to the end of synthesis (MBq; in SI, Bq); *RCY* is the radiochemical yield expressed as a dimensionless fraction (0–1); and n is the amount of precursor added (nmol; in SI, mol; 1 MBq/nmol = 1.0 × 10^{15} Bq/mol). For example, A = 30.8 MBq (decay-corrected to the end of synthesis), *RCY* = 0.982, and n = 0.7 nmol give A_m = 43.2 MBq/nmol. For reference, the theoretical molar activity of carrier-free ^{44}Sc is 2.92 × 10^4 MBq/nmol.

Determination of oxalate

After conditioning, the resulting ^{44}Sc solutions (typically 1 M sodium acetate, pH 4.00 ± 0.15) were analyzed for oxalate by ion chromatography with UV detection. Analyses were performed on a LicArt-62 chromatograph (Labconcept LLC, Saint Petersburg, Russia) with a Shodex IC SI-90 4E column (4.0 mm × 250 mm; Shodex Group, Tokyo, Japan) and a diode-array detector at 210 nm. The column temperature was 33 °C and the isocratic eluent (1.5 mL/min) was 1.8 mM Na_2CO_3 + 1.7 mM $NaHCO_3$. The retention times were 22.8 ± 0.2 min for oxalate and 1.31 ± 0.2 min for acetate. The limit of quantification for oxalate in the acetate matrix, determined by this method, was 1.6 × 10^{-3} M.

Calibration was linear over 1.6×10^{-3}–3.0×10^{-2} M ($r^2 = 0.996$), and the recovery of oxalate spiked into 1 M sodium acetate was 98–110 %. Samples were diluted four-fold before injection to keep the acetate peak within the linear range of the detector; the dilution was accounted for in the reported limit. Each solution was analyzed in six replicates.

Statistics

Results are presented as arithmetic mean ± sample standard deviation for $n = 5$ independent replicates, unless stated otherwise. Pairwise comparisons were made using Welch's t-test, which does not assume equal variances; for the simultaneous comparison of the nine resins, p values were adjusted using the Holm procedure. Differences were considered significant at $p < 0.05$. Rank correlation was assessed using Spearman's coefficient. All calculations were performed using OriginPro 2018 (OriginLab, Northampton, MA, USA).

Results

Selection of resin

Nine cation-exchange resins used for the purification or pre-concentration of scandium radioisotopes [9,28,39,41,42] were compared. In the established scheme, sorption proceeds from dilute HCl (0.1 M) and desorption from ammonium or sodium acetate (0.75–1.0 M, pH 4–5). Accordingly, $D_g(^{44}Sc)$ was determined in 0.1 M HCl, and in 1.0 M sodium acetate (pH 4.00 ± 0.15), and in the undiluted generator eluate (Fig. 1).

Chromafix HR-XC, Chromabond PSA, and Strata-X-C showed high sorption from 0.1 M HCl; the value obtained for OASIS MCX CC in this medium lies above the limit of quantification defined by Eq. (2) and is reported as censored ($D_g > 6.6 \times 10^3$ mL/g). In 1.0 M sodium acetate the lowest D_g values were obtained for Chromafix HR-XC and Chromabond PSA (7.0 ± 0.8 and 3.3 ± 0.6 mL/g). These two resins therefore combine strong retention with efficient release.

The third series in Fig. 1 shows $D_g(^{44}Sc)$ measured directly in the undiluted generator eluate. For seven of the nine resins, the values fall to 2–9 mL/g, that is, two to three orders of magnitude below those in 0.1 M HCl. Two resins deviated from this pattern. Chromabond PSA retains a comparatively high value (61 ± 7 mL/g), which is the basis of its behavior in column mode. AG MP-50 shows the opposite anomaly: its D_g in the eluate (809 ± 11 mL/g) exceeds that in 0.1 M HCl (96 ± 4 mL/g) by more than eightfold. A third observation concerns Sep-Pak Accell Plus CM, for which D_g increases from 5.0 ± 0.3 mL/g in 0.1 M HCl to 211 ± 5 mL/g in 1 M sodium acetate, the reverse of the behavior of every strong exchanger examined. Both deviations are addressed in the Discussion.

Effect of oxalate and hydrochloric acid

Since the generator eluent contained 0.1 M oxalic acid, sorption was studied in dilute HCl containing oxalate. Oxalate markedly impairs ^{44}Sc sorption on cation-exchange resins [33,34]: for Chromafix HR-XC, D_g was 1154 ± 80 mL/g in 0.1 M HCl but 12 ± 3 mL/g in 0.1 M HCl/0.1 M $H_2C_2O_4$, and 9 ± 2 mL/g in the generator eluate itself (0.2 M HCl/0.1 M $H_2C_2O_4$) (Table 1). Within the range examined at 0.1 M oxalic acid, the HCl concentration had no systematic effect on D_g (12 ± 3, 9.0 ± 0.6, and 8.0 ± 0.5 mL/g at 0.1, 0.05, and 0.01 M HCl; Welch's test, p = 0.27 for 0.1 vs 0.01 M, p = 0.021 for 0.05 vs 0.01 M). In contrast, at lower oxalate concentrations, acidity becomes important: at 0.005 M $H_2C_2O_4$, D_g was 1376 ± 144 mL/g in 0.2 M HCl (Table 1) but approximately 4×10^3 mL/g in 0.01 M HCl (Table 1). This dependence explains the difference between the present data and those of Pruszyński et al. [31], who worked at 0.07 M HCl.

The dependence of D_g on the dilution factor is shown in Fig. 2 for both selected resins. At 10-fold dilution, the value for Chromafix HR-XC approaches that measured in 0.1 M HCl (1062 ± 258 vs. 1154 ± 80 mL/g), and for Chromabond PSA it exceeds it (4730 ± 1221 vs. 2300 ± 793 mL/g); the

values obtained at 20-fold dilution lie above the limit defined by Eq. (2) and are reported as censored. Because the eluate volume is 1 mL, 10-fold or greater dilution increases both the working volume and the volume of liquid waste, and therefore, 5-fold dilution was adopted.

Column experiments

Column data (Fig. 3) were consistent with the batch values for seven of the nine resins. From the undiluted eluate, ^{44}Sc was retained with low efficiency on all cation-exchange resins, except Chromabond PSA. Fivefold dilution increased sorption above 95 % for six of the nine resins, to values comparable with those from 0.1 M HCl; for Strata-X-CW and Sep-Pak Accell Plus CM, dilution did not improve retention. OASIS MCX CC and Chromalite CGC 50×2 gave high retention from both the diluted eluate and 0.1 M HCl, whereas the Sep-Pak Accell Plus CM was unsuitable (42.6 ± 6.8 % from 0.1 M HCl) and was not studied further.

The dependence of ^{44}Sc sorption on Chromafix HR-XC on the dilution factor (Fig. 4) shows a plateau of quantitative sorption at fivefold dilution (98.4 ± 1.1 %), with no further gain on additional dilution ($p > 0.05$).

Chromabond PSA was examined further because it was the only resin to retain ^{44}Sc quantitatively from the undiluted eluate, which eliminates the dilution step altogether. Its D_g in the undiluted eluate exceeds that of Chromafix HR-XC by more than sixfold (61 ± 7 vs. 9 ± 2 mL/g). Sorption increased with bed mass and reached a plateau at ≥ 100 mg (99.0 ± 0.5 %; Fig. 5). All data in Fig. 5 were obtained on 100 × 2.1 mm columns, as the 50 mm format could not hold 200 mg of resin. Subsequent experiments used 100 mg of Chromabond PSA, which completely filled a 50 × 2.1 mm PEEK column.

Sodium acetate was selected for desorption. D_g measurements (Fig. 6A, B) showed that efficient release requires 1.0 M sodium acetate at pH 4.00 ± 0.15, where the lowest values were obtained for Chromabond PSA and Chromafix HR-XC (3.3 ± 0.6 and 7.0 ± 0.8 mL/g). Dynamic desorption (Table 2) confirmed the highest recovery for both resins under these conditions.

The batch and column data were not fully congruent at pH 5, where the two resins had similar D_g (14.0 ± 0.8 and 12 ± 2 mL/g) but very different dynamic recoveries (3 ± 1 % and 65 ± 7 %). This discrepancy is addressed in the Discussion and is resolved by the breakthrough volume of the two beds (Table 3).

With the eluent established, ^{44}Sc was desorbed from the other exchangers (Fig. 7). Four resins gave recoveries above 70 % (hatched bars in Fig. 7): Chromabond PSA (80.4 ± 2.7 %), AG MP-50 (85.8 ± 7.4 %), Chromafix HR-XC (76.3 ± 6.9 %), and Bond Elut SCX (75.3 ± 14.8 %). The recovery of Chromafix HR-XC was determined a second time, in the carboxylate-eluent series, as 79.4 ± 1.7 %

(Fig. 10); the two determinations did not differ (Welch's test, p = 0.38), and the value from the carboxylate series was the one used in the combined criterion below, since both factors of that product must originate in the same campaign. Strata-X-CW was not carried through to this stage, having retained only 30.2 ± 5.1 % of the applied activity at the sorption step (Fig. 3, best case, from 0.1 M HCl). Strata-X-C, by contrast, sorbs ^{44}Sc quantitatively but releases only 10.2 ± 2.5 % in 1 mL — the value predicted from its batch data: with D_g = 33 ± 4 mL/g in 1 M sodium acetate (Fig. 1) and a bed of 66 mg (Table 4), the breakthrough volume is ≈ 2.2 mL, more than twice the intended elution volume, so that most of the activity has not left the column when elution is stopped. The same reasoning applies to OASIS MCX CC, for which V_b = 2.4 mL in 1 M sodium acetate at pH 4.00 ± 0.15 and the observed recovery was 27.7 ± 4.3 %. In both cases, the batch method predicted the column failure prospectively. For AG MP-50, the eluate is acidified (pH 2.90 ± 0.13; raw pH data are provided in Supplementary Information: Table S3), requiring adjustment to pH 4.0–4.5 before labelling. Bond Elut SCX gave unstable recoveries (60–90 %). Chromabond PSA and Chromafix HR-XC gave consistent recoveries and solutions that can be used directly.

The elution profiles for the four resins (Fig. 8) show that 74–86 % of the activity is recovered in the first 1 mL. Increasing the volume of 1 M sodium acetate to 2 mL raises the recovery by 6–11 percentage points but lowers the activity concentration; therefore, elution with 1 mL was adopted. Figs. 7 and 8 were obtained in independent series and agreed within 2.1 % for every resin.

Activity balance

In column experiments, the activity balance was closed to 98.5 ± 1.0 % of the applied ^{44}Sc activity (decay-corrected; mean ± SD, n = 5) across the resins, accounting for essentially all of it. Sorption losses averaged 1.8 ± 1.5 % (with 1.0 ± 0.5 % for Chromabond PSA). For Bond Elut SCX, AG MP-50, Chromafix HR-XC, and Chromabond PSA, which exhibited high desorption yields (79.5 ± 4.8 % on average), the mean column retention loss was 18.3 ± 5.2 %. In contrast, Strata-X-C, Chromalite CGC 50×2, and Oasis MCX CC showed poor ^{44}Sc recovery (35.5 ± 29.9 % on average), with mean losses of 59.9 ± 31.7 %. Wash losses were negligibly small ((22 ± 6) × 10^{-5} %) and were therefore omitted from the balance calculation. The activity balance for each resin is presented individually in Table 5.

Purity of the conditioned solution

Oxalate was determined in the conditioned solutions using ion chromatography. The concentration fell from 0.1 M in the generator eluate to below the limit of quantification of 1.6 × 10^{-3} M, corresponding to a decontamination factor greater than 60 and to less than 1.6 µmol of oxalate in the 1 mL product, against 100 µmol applied to the column (n = 6 for each resin). In contrast to earlier reports [31, 34], where oxalate removal was inferred solely from the restoration of labelling

capability, the absence of residual oxalate in the conditioned ^{44}Ti/^{44}Sc generator eluate was confirmed here by direct measurement.

The analytical limit and labelling data together define the working tolerance of the process. At most 1.6 μmol of oxalate remains in the 1 mL product — a 1600-fold molar excess over the 0.96 nmol of PSMA-617 used and a 2500-fold excess over the 0.63 nmol of FAP-2286 — and yet radiochemical yields of 96.6–98.2 % were obtained, whereas labelling directly in the undiluted eluate (0.1 M oxalate, a 2×10^4-fold excess) is not possible. Therefore, the conditioning step does not have to remove oxalate completely; it has to bring the concentration below the level at which oxalate competes effectively with DOTA, and the present data place that level at or above 1.6×10^{-3} M. Notably, this experimental bound is transferable to other conditioning procedures.

^{44}Ti was not detected in any of the conditioned solutions using low-background γ-spectrometry. The activity expected in 1 mL of generator eluate, calculated from the breakthrough of 4.1×10^{-7} % (for the new prototype used in this work), is approximately 0.2 Bq; the minimum detectable activity of the method used was 14×10^{-3} Bq, so that the decontamination factor of the conditioning step for ^{44}Ti was greater than 14. The ^{44}Ti content of the product is therefore below 14×10^{-3} Bq per 1 mL, that is, below 4.5×10^{-8} % of the ^{44}Sc activity, which is more than four orders of magnitude below the parent-breakthrough limit (1×10^{-3} %) applied to ^{68}Ge/^{68}Ga generator eluates in the European Pharmacopoeia [43].

Synthesis of radiopharmaceuticals

The ^{44}Sc eluates from the four selected resins were used to prepare [^{44}Sc]Sc-PSMA-617 (Fig. 9), with 4.78 nmol of precursor. Elution of Bond Elut SCX with 5 M NaCl/0.13 M HCl has been reported to support > 95 % labelling of [^{44}Sc]Sc-DOTANOC [28]. Substituting 1 M sodium acetate, which avoids the osmotic penalty of the eluate, resulted in low and irreproducible yields (63.5 ± 18.6 % at 30 min). The eluate from AG MP-50, after adjustment to pH 4.00 ± 0.15, gave a high yield (98.1 ± 1.5 % at 20 min); however, the additional pH correction is a practical disadvantage. Chromabond PSA and Chromafix HR-XC gave high yields at 20 min (96.3 ± 2.0 % and 97.9 ± 1.4 %, respectively) and were selected for the subsequent experiments.

[^{44}Sc]Sc-DOTA-TATE and the FAP-targeting agent [^{44}Sc]Sc-FAP-2286 (Supplementary Information: Fig. S1) were prepared under the same conditions as [^{44}Sc]Sc-PSMA-617 (Fig. 9): 95 °C, 20 min, 1 M sodium acetate (pH 4.00 ± 0.15), total volume 1 mL. However, in this series of experiments, the amount of precursor was reduced — V_p = 1 μL of a 1 mg/mL precursor solution — and [^{44}Sc]Sc-PSMA-617 was synthesized under the same reduced-precursor conditions. The yields, radiochemical purities, and apparent molar activities are summarized in Table 6.

The three apparent molar activities were obtained at a mean product activity of 32.6 ± 0.3 MBq, decay-corrected to the end of synthesis; the calculated balance of Table 7 gives 32.9 MBq for the same point, so that the measured and calculated activities agree to within 0.9 %. The highest value, 50.0 ± 1.2 MBq/nmol for [^{44}Sc]Sc-FAP-2286, corresponds to 0.17 % of the theoretical molar activity of carrier-free ^{44}Sc and was obtained with 0.63 nmol of precursor (1 µL of 1 mg/mL solution: 0.63 nmol). Since 96.6 % of the activity was incorporated into 0.63 nmol of FAP-2286, the total amount of cations competing for the DOTA cavity in the 1 mL product cannot exceed the order of 0.63 µmol/L, equivalent to less than 35.3 µg/L expressed as iron. This is a bound rather than a measurement and is not a substitute for an elemental profile. The yield at 0.63 nmol was still 96.6 %, so the plateau of the molar-activity curve had not been reached: the value of 50.0 MBq/nmol is set by the precursor amount chosen and not by the quality of the ^{44}Sc solution.

Alternative buffer systems

Sodium salts of pharmaceutically acceptable mono- and dicarboxylic acids [44] were evaluated as alternatives to acetate, both as desorption agents and as media for subsequent labelling (Figs. 10, 11); sodium α-hydroxyisobutyrate [23] was also examined. All solutions were adjusted to pH 4.00 ± 0.15 and experiments were conducted using Chromafix HR-XC.

Desorption recoveries in 1 mL at 1.0 M (Fig. 10) decreased in the order malate (92.2 ± 2.9 %) > succinate (91.2 ± 1.5 %) > lactate (90.1 ± 3.9 %) > pyruvate (86.4 ± 2.1 %) ≈ α-HIB (86.2 ± 2.2 %) > acetate (78.9 ± 4.2 %). Acetate was thus the least effective of the six eluents over the whole concentration range, while succinate and malate were the most effective.

The eluates were then evaluated for the synthesis of [^{44}Sc]Sc-DOTA-TATE (Fig. 11). At the lowest concentration examined (0.2 M), the radiochemical yield decreased in the order acetate (99.4 ± 0.4 %) > pyruvate (97.5 ± 1.1 %) > succinate (95.4 ± 1.7 %) > lactate (91.5 ± 2.5 %) > α-HIB (39.2 ± 2.3 %) > malate (12.8 ± 1.8 %), and for every ligand except acetate, the yield fell steeply with increasing concentration. Sodium acetate gave yields ≥ 99 % across the entire concentration range.

Because desorption and labelling respond to buffer concentration in opposite directions, the two datasets were combined into a single figure of merit, $Y_{comb} = Y_{des} \times RCY$, evaluated at all 30 combinations of ligand and concentration (Fig. 12). The global maximum was 1 M sodium acetate (Y_{comb} = 78.8 ± 1.7 %), followed by 0.4 M succinate (72.1 ± 3.3 %), 0.8 M acetate (71.1 ± 1.9 %), and 0.6 M pyruvate (69.6 ± 3.3 %). Sodium acetate at 1 M was therefore adopted, notwithstanding its position as the weakest of the six eluents on desorption alone. The difference from the nearest alternative was 6.7 percentage points and was statistically significant (Welch's test, $t = 4.04$, $d_f = 6$, $p = 0.007$), so the choice was not marginal.

Discussion

The clinical adoption of scandium radioisotopes requires simple and reproducible methods of separation and purification. DGA resin is often preferred because it delivers scandium in dilute HCl [13,14,32,45], but the final volume of 4–5 mL gives a low activity concentration and consequently requires larger precursor amounts to reach a given apparent molar activity. Cation-exchange resins combine removal of oxalate with concentration into 1–3 mL and are well suited to the post-processing of ^{44}Ti/^{44}Sc generator eluates. For the activities handled here, the difference is a factor of four to five in activity concentration: approximately 31 MBq in 1 mL against the same activity distributed over 4–5 mL.

Sorption behavior

The D_g data show that decreasing the oxalate concentration markedly increases sorption, and fivefold dilution enables quantitative retention for most resins examined. This is consistent with Pruszyński et al. [31], who achieved 96 % sorption on 80 mg of AG 50W×8 from 0.005 M $H_2C_2O_4$/0.07 M HCl; the present data extend the accessible range to a fourfold higher oxalate concentration (0.02 M).

Chromabond PSA retains ^{44}Sc quantitatively from the undiluted eluate at 0.1 M oxalic acid. The effect follows directly from the breakthrough volume of the bed, $V_b \approx D_g \cdot m$, with D_g = 61 mL/g and 100 mg of resin, $V_b \approx 6.1$ mL, sixfold the 1 mL sample volume, so that the sample is loaded well inside the retention capacity of the column. The same calculation reproduces the observed behavior of Chromafix HR-XC both undiluted ($V_b \approx 0.57$ mL, $V_s/V_b = 1.8$, partial breakthrough, 45.5 ± 5.4 % retention) and after fivefold dilution ($V_b \approx 16.9$ mL, $V_s/V_b = 0.30$, 98.4 ± 1.1 % retention), where V_s is the volume of the sample solution loaded (1 mL and 5 mL, respectively). All breakthrough volumes in Table 4 are calculated from D_g measured in the undiluted eluate, which is the medium applied to the column in the scheme of Fig. 13B.

AG MP-50 and Sep-Pak Accell Plus CM cation-exchange resins show contrasting sorption behavior. AG MP-50 is the only macroporous styrene–divinylbenzene material in the set, and it is the only resin whose D_g increases in the oxalate medium (809 ± 11 mL/g) relative to 0.1 M HCl (96 ± 4 mL/g). At 0.1 M oxalic acid, Sc(III) is present predominantly as neutral and anionic oxalato species, which cannot be retained by cation exchange; however, retention on a macroporous hydrophobic matrix by adsorption is available to such species. The consequence is a mixed-mode retention in which the adsorption channel dominates in the batch experiment. The channel is slow: over 24 h of equilibration produces a high apparent D_g, whereas at a linear flow corresponding to 1 mL/min, it does not have time to operate, and the column retains only 35.6 ± 3.7 % of the applied activity (Fig. 3). The batch and column data for AG MP-50 are therefore not contradictory but report on two different retention

mechanisms operating on different timescales. The practical implication is that the D_g measured in oxalate media on macroporous polymeric supports is not transferable to column design.

Sep-Pak Accell Plus CM behaves in the opposite manner, and for a straightforward reason. Its carboxymethyl group is a weak acid ($pK_a \approx 4.5–5$). In 0.1 M HCl it is fully protonated, and no ion exchange is possible, giving $D_g = 5.0 \pm 0.3$ mL/g and a breakthrough volume of 0.37 mL, which quantitatively accounts for the 42.6 ± 6.8 % retention observed from a 1 mL sample. In 1 M sodium acetate at pH 4.00, the group is partly ionized, and D_g rises to 211 ± 5 mL/g. Thus, the resin is unusable in the present scheme, but its behavior confirms that the batch method responds correctly to the ionization state of the functional group and provides an internal control for D_g measurements.

Increasing the resin mass could similarly help other exchangers: Pruszyński et al. obtained 99.9 % retention on 200 mg of AG 50W×8 [31]. However, more sorbent requires a larger eluent volume, lowering the activity concentration — illustrated by a recent ^{47}Sc study [25] in which 1.5 g of AG MP-50 required 40 mL of 1 M ammonium acetate for 93.7 ± 5.6 % recovery, whereas in the present study, 85 mg and 1 mL of 1 M sodium acetate gave 85.8 ± 7.4 % (Fig. 7). Dilution with water is thus a simpler and more predictable route to high retention.

The limit to that argument is stoichiometric and can be stated quantitatively. One milliliter of 1 M sodium acetate delivers 1 mmol of Na^+ to the column, whereas the total exchange capacity of the bed is the product of the nominal capacity (Supplementary Information: Table S2) and the mass (Table 4). For the resins used here, the ratio of delivered Na^+ to bed capacity is 14.3 for Chromabond PSA, 15.9 for Chromafix HR-XC, 14.1 for OASIS MCX CC, and 11.9 for Bond Elut SCX, but only 1.03 for Chromalite CGC 50×2, whose nominal capacity is 5.0 meq/g. This resin operates at the stoichiometric boundary: the eluent barely provides one equivalent of competing cation per equivalent of fixed charge, and its recovery of 68.5 ± 3.9 % cannot be improved without a proportional increase in the eluent volume. The same arithmetic explains why 1.5 g of AG MP-50 required 40 mL of the eluent in [25]. Therefore, a low nominal capacity is therefore a design requirement rather than a deficiency when the objective is elution into a minimal volume, and it is the principal reason for preferring Chromabond PSA (0.7 meq/g) over the high-capacity gel resins. A high ratio is necessary but not sufficient: OASIS MCX CC has a favorable ratio but recovers only 27.7 ± 4.3 %, which points to an additional, presumably mixed-mode, retention contribution of the kind discussed above for AG MP-50.

The batch method has clear limitations as a predictor of column behavior. It reproduces the column data for the two selected resins at the sorption step, and predicts the poor recovery at the desorption step (e.g., Strata-X-C: 10.2 ± 2.5 % against a breakthrough volume of 2.2 mL for a 1 mL elution). However, it fails for Strata-X-CW, where $D_g = 319 \pm 50$ mL/g in 0.1 M HCl predicts near-quantitative

retention, while 30.2 ± 5.1 % was observed. Since the resins were used as supplied, without conversion to a defined ionic form, and because the sorption kinetics were not characterized, D_g is best regarded here as a screening tool rather than as a predictive model of the column.

The apparent batch–column discrepancy at pH 5

The divergence noted in the Results — two resins with almost identical distribution coefficients at pH 5 (14.0 ± 0.8 and 12 ± 2 mL/g), but recoveries differing 22-fold (3.1 ± 0.8 % and 65.4 ± 7.1 %) — resolves once the bed masses of Table 4 are considered. What governs elution in a fixed volume is not D_g, but the breakthrough volume $V_b = D_g \cdot m$, and the two beds differ in mass by a factor of 1.6. At pH 5, Chromabond PSA (100 mg) gives V_b = 1.40 mL, so that a 1 mL eluent volume stops short of the breakthrough point and almost nothing is recovered; Chromafix HR-XC (63 mg) gives V_b = 0.76 mL, so that elution is already well advanced after 1 mL. The same calculation accounts for the behavior at pH 4 and pH 6 for both resins (Table 3). Only at pH 3 for Chromafix HR-XC does the observed recovery exceed the prediction, which is consistent with an additional displacement channel — competition by protons for the sulfonic sites — that lies outside the breakthrough-volume framework. Seven of the eight pH points are thus described by a single relation, and the apparent contradiction at pH 5 is an artifact of comparing D_g values measured on beds of different mass.

Desorption and choice of eluent

As reported by Pietrelli et al. [21], Sc(III) is so strongly retained on strong cation-exchange resins, and desorption requires a complexing agent; they proposed acetic acid/ammonium acetate (pH 4.7). Here 1 M sodium acetate (pH 4.00 ± 0.15) was used. Bond Elut SCX is normally eluted with ≈ 5 M NaCl/0.1 M HCl (≥ 95 % in 700 µL), but the calculated osmolality of that eluate, ≈ 9.9 osmol/kg, precludes direct administration [27]; sodium acetate allows direct use but gives inconsistent recovery (60–90 %) and erratic labelling (63.5 ± 18.6 %) at 30 min (Fig. 9). AG MP-50 acidifies the eluate and requires pH adjustment. Chromabond PSA and Chromafix HR-XC gave solutions suitable for high-yield synthesis, and two post-elution processing schemes were assembled from these results (Figs. 13A, B).

For the first post-elution processing scheme (fivefold diluted eluate loaded onto the column, Fig. 13A), the total flow time at f = 1 mL/min was 8 min. Including manual handling and activity measurement, the overall processing time was at most 15 min (13.5 ± 1.5 min, n = 5). For the second scheme (undiluted eluate, Fig. 13B) the flow time was 4 min, giving at most 11 min under the same handling conditions (9 ± 2 min, n = 5). The steps involved are of the kind normally implemented in automated synthesis modules, although no automated implementation was carried out in this study. Because the 4 min difference corresponds to less than 2 % of the ^{44}Sc half-life and lies within the variability of manual operations, a conservative decay correction of 15 min was applied uniformly to

both schemes so that the radiochemical yields remained comparable. The ^{44}Sc solution in 1 M sodium acetate was suitable for high-yield labelling of [^{44}Sc]Sc-PSMA-617 and [^{44}Sc]Sc-DOTA-TATE using 0.96 and 0.7 nmol of precursor, respectively; for [^{44}Sc]Sc-FAP-2286, the same conditions gave a yield of 96.6 ± 2.3 % with as little as 0.63 nmol.

The overall efficiency of the process can be estimated from the individual steps (Table 7). With an elution yield of 95.6 %, a sorption of 99 %, desorption of 80.4 %, and allowing for decay during processing, 69.0 % of the ^{44}Sc present on the generator is delivered to the reaction vessel, and 66.8 % is present in the product at the end of a 20 min synthesis. Table 7 presents a calculated cross-check of the measured activities, and is not the source of any value reported in Table 6; the two agree to within 0.9 %.

The conditioned solution is an intermediate for labelling and not a finished dosage form. One milliliter of 1 M sodium acetate adjusted to pH 4.00 with hydrochloric acid contains approximately 1 M Na^+, 0.15 M acetate, 0.85 M chloride, and 0.85 M acetic acid, with a calculated osmolality of ≈ 2.8 osmol/kg; dilution or reformulation would be required before administration. The same consideration applies, more strongly, to the 4.8 M NaCl medium discussed above.

Choice of the auxiliary ligand

In the labelling of macrocyclic chelators with scandium, the metal must be kept in a form that remains accessible to the macrocycle. Sc^{3+} has a small ionic radius (0.745 Å for coordination number 6 [46]) and a high charge density, and therefore hydrolyses readily. At ultratrace metal concentrations during radiochemical synthesis, polynuclear hydroxo species are unimportant, and the dominant factor is the competition between the auxiliary ligand of the buffer and the DOTA macrocycle. A ligand that binds too weakly does not protect the metal from hydrolysis; one that binds too strongly forms a thermodynamic trap and retards labelling [47].

Because all experiments were carried out at pH 4.00, the tabulated stability constants of the fully deprotonated ligands (Supplementary Information: Table S4 [48–51]) cannot be compared directly. The relevant quantity is the conditional constant, $K_1' = \alpha_L \cdot K_1$, where α_L is the fraction of the ligand present in the fully deprotonated form:

$$\alpha_L = [1 + \Sigma_i \Pi_j 10^{(pKa,n-j+1 - pH)}]^{-1} \quad (4)$$

Table 8 lists the values of α_L and the product $K_1 \cdot [L]$ at pH 4.00 for the six ligands studied. The key consequence is that a nominally 1 M acetate buffer at pH 4.00 contains only 0.148 M acetate ions, the remainder being undissociated acetic acid, whereas pyruvate (pK_a 2.49) is 97% dissociated. The observed ranking of the labelling yields is inversely related to $\log(K_1 \cdot [L])$ across the series (Spearman $\rho = -0.83$, $n = 6$); the sign is negative because a stronger auxiliary complex gives a lower yield, and

the same quantity accounts for the ranking of desorption recoveries in the opposite direction. The two rankings are therefore governed by one variable, which is why an eluent cannot be optimized on desorption alone and why the combined criterion of Fig. 12 is required.

Acetate is the weakest competitor of the six under the conditions used. It provides essentially electrostatic coordination without intramolecular chelation; therefore, the $[Sc(OAc)_n]^{3-n}$ species is kinetically labile, and DOTA readily intercepts the metal, yielding ≥ 99 % at every concentration examined.

Pyruvate coordinates weakly through the α-carbonyl group, which does not create a significant chelate barrier, and transchelation proceeds almost as rapidly as with acetate at low concentrations.

Succinate binds as a bidentate ligand through two carboxylate groups, forming a seven-membered ring. Its apparent advantage at low concentration is a consequence of protonation rather than of weak binding: at pH 4.00 only 0.87 % of succinate is present as the dianion, so the effective competitor concentration is low and the equilibrium is displaced towards free Sc^{3+}, which DOTA then scavenges.

Lactate closes a five-membered chelate ring through the α-hydroxy group, which introduces kinetic resistance; higher temperatures or longer incubation times are required for high yield.

α-Hydroxyisobutyrate carries two methyl groups whose inductive and steric (Thorpe–Ingold) effects strengthen the chelate ring relative to lactate (log K_1 = 4.84), and the labelling rate decreases further. Kurakina et al. [23] obtained both high desorption (95 ± 3 % in ≈300 µL of 0.1 M NH_4-α-HIB, pH 4.8) and high labelling (98 %) for [^{44}Sc]Sc-DOTA and [^{44}Sc]Sc-DOTATOC, but with an additional 0.1 M NaOAc buffer and an aliquot of 1 MBq, so that the final α-HIB concentration was 0.02 M. In the present study, lowering the Na-α-HIB concentration to 0.2 M raised the labelling yield to 39.2 ± 2.3 % while reducing desorption to 77.8 ± 2.6 %, so that no combination of the two was competitive.

Malate combines two carboxylate groups and one hydroxyl group and can encapsulate Sc^{3+} in a fused five- and six-membered ring system, giving the deepest well of the series and the lowest labelling yield. Tartrate and citrate, which form even more stable complexes (log β_1 > 17), were not tested here and are cited only for context.

Reliable experimental constants for scandium complexes of pyruvate and malate are not available; the values used in Table 8 were estimated from structural and thermodynamic analogy, as described in Supplementary Information: Table S4, and are identified as such. The conclusions of this section do not depend on the exact magnitude of the values, only on their rank order.

Limitations of the study

The following limitations define the scope of the conclusions drawn in this study.

The chemical purity of the conditioned ^{44}Sc was not characterized, and no ICP-MS metal-ion profile was obtained. Trace Fe, Zn, Cu, Ti, Al, and Ca compete with Sc(III) for the DOTA cavity and set the ceiling on the achievable apparent molar activity. An indirect upper bound follows from the data presented: successful labelling of 0.63 nmol of FAP-2286 at 96.6 % yield limits the total amount of DOTA-competing cations in 1 mL of product to the order of 0.63 nmol.

The absence of ^{44}Ti in the conditioned solution is established as an upper bound set by the detection limit of the γ-spectrometric method; the decontamination factor of the column for ^{44}Ti was not determined independently, since the ^{44}Ti activity in the eluate itself (≈ 0.2 Bq) is close to that limit.

Residual oxalate is reported as below the limit of quantification of the ion-chromatographic method (1.6×10^{-3} M); the method was validated for the acetate matrix used here but not for the other carboxylate media examined in Figs. 10 and 11. Because that limit is 1.6 % of the concentration in the eluate, the analytical evidence establishes removal of at least 98.4 % rather than complete removal; the functional bound set out in the Results extends the conclusion but does not replace a determination at a lower limit.

Apparent molar activity was determined at single precursor amounts; no titration against the precursor amount was performed, and no plateau was established; therefore, the highest value reported (50.0 MBq/nmol, 0.17 % of the theoretical value) is a lower bound on what the solution can support.

Distribution coefficients above 6.6×10^3 mL/g lie beyond the limit of quantification of the batch method at V/m = 66.7 mL/g and are reported as censored.

The sorption kinetics were not studied, and equilibrium at 24 h was assumed; the resins were used in the ionic form supplied, so comparisons of D_g between resins are relative. For macroporous polymeric supports in oxalate media the batch value additionally reflects a slow adsorption channel that does not operate under column conditions, as discussed above for AG MP-50.

Residual ethanol from the wash step was not determined (ICH Q3C class 3 limit 5000 ppm [52]).

Product identity was confirmed by radio-TLC only; HPLC was not performed, and the systems used do not resolve colloidal or hydrolyzed Sc(III) species separately.

The work was carried out at the prototype scale (nominal 50 MBq of ^{44}Ti); the complete sequence generator–conditioning–synthesis was not run as a single validated procedure, no automated implementation was made, and batch-to-batch reproducibility of the resins, column lifetime and the *in vitro* and *in vivo* stability of the products were not assessed.

Conclusions

Cation-exchange resins are effective for the post-elution processing of the TEVA-based ^{44}Ti/^{44}Sc generator eluate, combining oxalate removal with concentration in a minimal volume. Nine exchangers were compared under identical conditions, and two were selected. Quantitative sorption of ^{44}Sc is achieved either directly from the eluate (Chromabond PSA, 99.0 ± 0.5 %) or after fivefold dilution (Chromafix HR-XC, 98.4 ± 1.1 %), and desorption with 1 M sodium acetate (pH 4.00 ± 0.15) proceeds in 1 mL with recoveries of 80.4 ± 2.7 % and 76.3 ± 6.9 %, the activity balance of the column closing to 98.5 ± 1.0 %. The principal practical advantage of Chromabond PSA is not a higher recovery — the difference from Chromafix HR-XC is not statistically significant — but the elimination of the dilution step. Oxalate is removed by a factor greater than 60, to below 1.6×10^{-3} M, and ^{44}Ti remains below the detection limit of low-background γ-spectrometry (14×10^{-3} Bq, i.e. below 4.5×10^{-8} % of the ^{44}Sc activity); both were determined analytically rather than inferred. The resulting solution enables the labelling of DOTA conjugates, as shown for [^{44}Sc]Sc-DOTA-TATE, [^{44}Sc]Sc-PSMA-617, and the FAP inhibitor [^{44}Sc]Sc-FAP-2286, with a maximum apparent molar activity of 50.0 ± 1.2 MBq/nmol at 0.63 nmol of precursor; the yield of 96.6 ± 2.3 % at that amount indicates that the attainable molar activity was limited by the precursor loading rather than by the quality of the ^{44}Sc solution. Of six carboxylate eluents examined at five concentrations, 1 M sodium acetate was the global optimum of the combined desorption–labelling criterion (Y_{comb} = 78.8 ± 1.7 %**,** p = 0.007 against the nearest alternative), despite being the weakest of the six on desorption alone; the two rankings are governed by a single variable, the conditional stability of the auxiliary complex at pH 4.00, which is why neither criterion alone is sufficient. The schemes use only commercially available resins. The metal-ion profile of the product remains to be characterized before clinical translation can be considered. At the prototype scale examined here, the combination of the TEVA-based generator with cation-exchange conditioning provides a practical route to ^{44}Sc solutions of a quality sufficient for DOTA-conjugate labelling without a cyclotron on site.

List of abbreviations

PET — positron emission tomography; SPECT — single-photon emission computed tomography; SPE — solid-phase extraction; DOTA — 1,4,7,10-tetraazacyclododecane-1,4,7,10-tetraacetic acid; PSMA — prostate-specific membrane antigen; FAP — fibroblast activation protein; D_g — mass distribution coefficient; *RCP* — radiochemical purity; *RCY* — radiochemical yield; A_m — apparent molar activity; α-HIB — α-hydroxyisobutyrate; NaOAc — sodium acetate; TLC — thin-layer chromatography; ICP-MS — inductively coupled plasma mass spectrometry; EOS — end of synthesis; SD — standard deviation; V_b — breakthrough volume; V_s — sample volume; V_p — volume of precursor solution; f — flow rate; Y_{comb} — combined desorption–labelling criterion; MDA — minimum detectable activity; IC — ion chromatography

Declarations

Ethics approval and consent to participate: Not applicable (no human or animal subjects were involved).

Consent for publication: Not applicable.

Availability of data and materials: The datasets generated during this study are not publicly available due to the regulations of the Federal Medical Biological Agency of Russia governing state-assigned research; they may be obtained from the corresponding author upon reasonable request.

The raw data are available from the corresponding author on reasonable request.

Competing interests: The authors declare that they have no competing interests. The authors have no financial or other relationships with any of the manufacturers whose products were evaluated.

Funding: This work was carried out within the framework of the state assignment of the Federal Medical Biological Agency of Russia (R&D registration No. 125022502879-3).

Authors' contributions: PM and AL designed the study; PM performed the distribution-coefficient and column experiments, the radiosynthesis and the radio-TLC analyses and processed the data; AL performed the γ-spectrometric measurements and supervised the work; PM and AL drafted the manuscript and revised it critically. Both authors read and approved the final version.

Acknowledgements: Not applicable

Use of AI-assisted technologies: No artificial intelligence (AI)-assisted technologies, including large language models, generative AI, or AI-based editing tools, were used at any stage of the research, data analysis, or manuscript preparation.

Tables

Table 1. Distribution coefficient of ^{44}Sc on Chromafix HR-XC as a function of oxalic acid and hydrochloric acid concentrations (mean ± SD, mL/g; n = 5).

Oxalic acid, mol/L	HCl, mol/L	Dg(^{44}Sc), mL/g	Comment
0.1	0.1	12 ± 3	—
	0.05	9.0 ± 0.6	p = 0.021 vs. 0.01 M HCl
	0.01	8.0 ± 0.5	p = 0.27 vs. 0.1 M HCl
	0.2	9 ± 2	undiluted eluate
0.05	0.2	43.0 ± 3.8	—
0.01	0.2	766 ± 99	D_g(^{44}Sc) 1062 ± 258 at 0.02 M HCl
0.005	0.2	1376 ± 144	D_g(^{44}Sc) ≈ 4 × 10^3 at 0.01 M HCl

Table 2. Recovery of ^{44}Sc in 1 mL as a function of eluent pH (1 M sodium acetate; mean ± SD, %; n = 5), with the corresponding batch distribution coefficients.

Resin	Parameter	pH 3	pH 4	pH 5	pH 6
Chromafix HR-XC	Recovery, %	42.7 ± 4.3	76.3 ± 6.9	65.4 ± 7.1	27.2 ± 3.4
	D_g, mL/g	84 ± 12	7.0 ± 0.8	12 ± 2	36 ± 6
Chromabond PSA	Recovery, %	66.2 ± 4.0	80.4 ± 2.7	3.1 ± 0.8	0
	D_g, mL/g	5.0 ± 0.5	3.3 ± 0.6	14.0 ± 0.8	105 ± 7

Table 3. Breakthrough volume and observed recovery in 1 mL as a function of eluent pH (1 M sodium acetate).

Resin	pH	D_g, mL/g	m, mg	V_b, mL	Recovery in 1 mL, %	Agreement
Chromafix HR-XC	3	84 ± 12	63	5.3	42.7 ± 4.3	under-predicted
	4	7.0 ± 0.8	63	0.44	76.3 ± 6.9	yes
	5	12 ± 2	63	0.76	65.4 ± 7.1	yes
	6	36 ± 6	63	2.3	27.2 ± 3.4	yes
Chromabond PSA	3	5.0 ± 0.5	100	0.50	66.2 ± 4.0	yes
	4	3.3 ± 0.6	100	0.33	80.4 ± 2.7	yes
	5	14.0 ± 0.8	100	1.40	3.1 ± 0.8	yes
	6	105 ± 7	100	10.5	0	yes

Table 4. Column configurations used in the dynamic experiments, with breakthrough volumes calculated from D_g measured in the undiluted generator eluate (Fig. 1), and the ratio of the Na^+ delivered by 1 mL of 1 M sodium acetate to the total exchange capacity of the bed.

Resin	**Mass, mg**	**Column, mm**	**D_g in eluate, mL/g**	**$V_b = D_g \cdot m$, mL**	**Na^+ / capacity**
Chromabond PSA	100	50 × 2.1 (100 × 2.1 for Fig.5)	61 ± 7	6.1	14.3
Chromafix HR-XC	63	50 × 2.1	9 ± 2	0.57	15.9
AG MP-50	85	50 × 2.1	809 ± 11	68.7	7.84
Bond Elut SCX	105	50 × 2.1	3.0 ± 0.8	0.32	11.9
Strata-X-C	66	50 × 2.1	3.0 ± 0.7	0.20	15.2
Strata-X-CW	46	50 × 2.1	2.0 ± 0.3	0.09	29.4
OASIS MCX CC	71	50 × 2.1	4.0 ± 0.2	0.28	14.1
Chromalite CGC 50×2	195	50 × 2.1	7.0 ± 0.5	1.37	1.03
Sep-Pak Accell Plus CM	74	50 × 2.1	2.0 ± 0.3	0.15	36.5

Table 5. Activity balance of the column, by resin (mean ± SD, %, n = 5).

Resin	**Sorption loss, %**	**Retained on column, %**	**Recovered in 1 mL, %**	**Sum, %**
AG MP-50	0.6 ± 0.3	11.1 ± 7.4	85.8 ± 7.4	97.5 ± 0.4
Chromabond PSA	1.0 ± 0.5	18.3 ± 2.7	80.4 ± 2.7	99.7 ± 0.1
Chromafix HR-XC	1.6 ± 1.1	20.7 ± 6.9	76.3 ± 6.9	98.6 ± 0.5
Bond Elut SCX	0.6 ± 0.3	23.2 ± 14.8	75.3 ± 14.8	99.1 ± 0.2
Chromalite CGC 50×2	4.9 ± 4.4	24.4 ± 5.9	68.5 ± 3.9	97.8 ± 0.3
OASIS MCX CC	2.3 ± 1.2	69.8 ± 4.5	27.7 ± 4.3	99.8 ± 0.1
Strata-X-C	1.7 ± 0.5	85.4 ± 2.6	10.2 ± 2.5	97.3 ± 0.3

Table 6. Summary of the radiosyntheses performed with conditioned ^{44}Sc (95 °C, 20 min, 1 mL of 1 M sodium acetate, pH 4.00 ± 0.15).

Product	**V_p, µL**	**n, nmol**	***RCY*, %**	***RCP*, %**	***A*(EOS), MBq**	**A_m, MBq/nmol**	**n**
[^{44}Sc]Sc-PSMA-617	1	0.96	97.1 ± 1.1	≥ 97	32.8 ± 0.3	33.2 ± 0.5	5
[^{44}Sc]Sc-DOTA-TATE	1	0.7	98.2 ± 1.5	≥ 98	32.3 ± 0.5	45.3 ± 1.0	5
[^{44}Sc]Sc-FAP-2286	1	0.63	96.6 ± 2.3	≥ 96	32.6 ± 0.2	50.0 ± 1.2	5

Table 7. Calculated activity balance of the process for a generator with a measured ^{44}Ti activity of 49.2 MBq, 24 h after the preceding elution.

Stage	**Activity, MBq**	**Cumulative yield, %**
^{44}Ti activity at the time of measurement	49.2	—
44Sc on the generator at equilibrium (24 h)	48.5	98.5
After elution (95.6 %)	46.3	94.2
After sorption (99 %)	45.8	93.3
After desorption (80.4 %)	36.9	75.0
Corrected for decay during processing (15 min)	35.3	71.7
In the reaction mixture	34.9	70.9
Product at the and of synthesis (20 min)	32.9	66.8

Table 8. Degree of dissociation and conditional ligand availability at pH 4.00 for the six carboxylate eluents.

Ligand	**pK_a**	**A(L·n$^-$)**	**[L] at 1 M**	**log(K_1 [L]), 1 M**	**log(K_1 [L]), 0.2 M**
Acetate	4.76	0.148	0.148	2.65	1.95
Pyruvate	2.49	0.970	0.970	3.59*	2.89*
Lactate	3.86	0.580	0.580	3.53	2.83
α-HIB	3.79	0.619	0.619	4.63	3.93
Succinate	4.21 / 5.64	0.0087	0.0087	3.49	2.79
Malate	3.40 / 5.11	0.0584	0.0584	5.27*	4.57*

*Based on estimated stability constants (Supplementary Information: Table S4). Spearman ρ between *RCY* at 0.2 M and log(K_1·[L]) is −0.83 (n = 6).

References

1. Laboratoire National Henri Becquerel. Recommended data. Available at: http://www.lnhb.fr/nuclear-data/nuclear-data-table/ (accessed 9 December 2025). n.d.
2. Szücs D, Csupász T, Szabó JP *et al.* Synthesis, Physicochemical, Labeling and In Vivo Characterization of ^{44}Sc-Labeled DO3AM-NI as a Hypoxia-Sensitive PET Probe. *Pharmaceuticals* 2022;**15**(6):666. https://doi.org/10.3390/ph15060666.
3. Singh A, Meulen NP van der, Müller C *et al.* First-in-human PET/CT imaging of metastatic neuroendocrine neoplasms with cyclotron-produced 44Sc-DOTATOC: a proof-of-concept study. *Cancer Biother Radiopharm* 2017;**32**(4):124–32. https://doi.org/10.1089/cbr.2016.2173.
4. Becker K V., Aluicio-Sarduy E, Bradshaw T *et al.* Cyclotron production of ^{43}Sc and ^{44g}Sc from enriched ^{42}CaO, ^{43}CaO, and ^{44}CaO targets. *Front Chem* 2023;**11**. https://doi.org/10.3389/fchem.2023.1167783.
5. Gomes CV, Mendes BM, Paixão L *et al.* Comparison of the dosimetry of scandium-43 and scandium-44 patient organ doses in relation to commonly used gallium-68 for imaging neuroendocrine tumors. *EJNMMI Phys* 2024;**11**(1):61. https://doi.org/10.1186/s40658-024-00669-5.
6. Siwowska K, Guzik P, Domnanich KA *et al.* Therapeutic Potential of ^{47}Sc in Comparison to ^{177}Lu and ^{90}Y: Preclinical Investigations. *Pharmaceutics* 2019;**11**(8):424. https://doi.org/10.3390/pharmaceutics11080424.
7. Glaser OM, Goerlach H, Salek M V. *et al.* Evaluation of Bifunctional, PSMA-Targeted Triazamacrocycle-Picolinates Compatible with the ^{18}F/ ^{44}Sc/ ^{177}Lu Isotope Triad. *J Med Chem* 2025;**68**(24):26234–45. https://doi.org/10.1021/acs.jmedchem.5c02286.
8. Mikolajczak R, Huclier-Markai S, Alliot C *et al.* Production of scandium radionuclides for theranostic applications: towards standardization of quality requirements. *EJNMMI Radiopharm Chem* 2021;**6**(1):19. https://doi.org/10.1186/s41181-021-00131-2.
9. Domnanich KA, Eichler R, Müller C *et al.* Production and separation of ^{43}Sc for radiopharmaceutical purposes. *EJNMMI Radiopharm Chem* 2017;**2**(1):14. https://doi.org/10.1186/s41181-017-0033-9.
10. Cingoranelli SJ, Bartels JL, Kankanamalage PHA *et al.* Production and purification of ^{43}Sc and ^{47}Sc from enriched [^{46}Ti]TiO_2 and [^{50}Ti]TiO_2 targets. *Sci Rep* 2023;**13**(1):22683. https://doi.org/10.1038/s41598-023-49377-7.
11. Meulen NP van der, Hasler R, Talip Z *et al.* Developments toward the Implementation of ^{44}Sc Production at a Medical Cyclotron. *Molecules* 2020;**25**(20):4706. https://doi.org/10.3390/molecules25204706.
12. Chernysheva M, Loveless SC, Brossard T *et al.* Accelerator production of scandium radioisotopes: Sc-43, Sc-44, and Sc-47. *Curr Radiopharm* 2021;**14**(4):359–73. https://doi.org/10.2174/1874471014999210112205535.
13. Schmidt CE, Gajecki L, Deri MA *et al.* Current State of ^{44}Ti/^{44}Sc Radionuclide Generator Systems and Separation Chemistry. *Curr Radiopharm* 2023;**16**(2):95–106. https://doi.org/10.2174/1874471016666221111154424.
14. Feng Y, Shao Y, Li Z *et al.* Research Progress on Major Medical Radionuclide Generators. *Processes* 2025;**13**(2):521. https://doi.org/10.3390/pr13020521.
15. Sammartano A, Migliari S, Scarlattei M *et al.* Performance and long-term consistency of five Galliform ^{68}Ge/^{68}Ga generators used for clinical Ga-68 preparations over a 4 year period. *Nucl Med Commun* 2022;**43**(5):568–76. https://doi.org/10.1097/MNM.0000000000001545.
16. Meiers JL, Foley A, Beattie C *et al.* Exploring rapid chemical separations of Sc-47 produced from photonuclear reactions on natural vanadium targets. *J Radioanal Nucl Chem* 2022;**331**(12):5623–30. https://doi.org/10.1007/s10967-022-08611-8.
17. Rotsch DA, Brown MA, Nolen JA *et al.* Electron linear accelerator production and purification of scandium-47 from titanium dioxide targets. *Appl Radiat Isot* 2018;**131**:77–82. https://doi.org/10.1016/j.apradiso.2017.11.007.

18. Kankanamalage PHA, Brossard T, Song J *et al.* Photonuclear production of ^{47}Ca for ^{47}Ca/^{47}Sc generator from natural $CaCO_3$ targets. *Appl Radiat Isot* 2023;**200**:110943. https://doi.org/10.1016/j.apradiso.2023.110943.
19. Valdovinos HF, Hernandez R, Barnhart TE *et al.* Separation of cyclotron-produced ^{44}Sc from a natural calcium target using a dipentyl pentylphosphonate functionalized extraction resin. *Appl Radiat Isot* 2015;**95**:23–9. https://doi.org/10.1016/j.apradiso.2014.09.020.
20. Misiak R, Walczak R, Wąs B *et al.* ^{47}Sc production development by cyclotron irradiation of ^{48}Ca. *J Radioanal Nucl Chem* 2017;**313**(2):429–34. https://doi.org/10.1007/s10967-017-5321-z.
21. Pietrelli L, Mausner LF, Kolsky KL. Separation of carrier-free ^{47}Sc from titanium targets. *J Radioanal Nucl Chem Artic* 1992;**157**(2):335–45. https://doi.org/10.1007/BF02047448.
22. Mehta VP, Khopkar SM. Cation Exchange Chromatographic Separation of Scandium from Other Elements on Dowex 50W-X8. *Sep Sci Technol* 1978;**13**(10):933–9. https://doi.org/10.1080/01496397808057139.
23. Kurakina ES, Wharton L, Hoehr C *et al.* Improved separation scheme for ^{44}Sc produced by irradiation of natCa targets with 12.8 MeV protons. *Nucl Med Biol* 2022;**104**–**105**:22–7. https://doi.org/10.1016/j.nucmedbio.2021.11.002.
24. Bartoś B, Majkowska A, Krajewski S *et al.* New separation method of no-carrier-added ^{47}Sc from titanium targets. *Radiochim Acta* 2012;**100**(7):457–62. https://doi.org/10.1524/ract.2012.1938.
25. Cingoranelli SJ, Putnam EE, Appiah JP *et al.* Production of high purity ^{47}Sc from proton irradiation of natural vanadium targets. *EJNMMI Radiopharm Chem* 2024;**9**(1):89.
26. Wojdowska W, Pawlak D, Cieszykowska I *et al.* Improved procedures of $Sc(OH)_3$ precipitation and UTEVA extraction for ^{44}Sc separation. *Nucl Med Rev* 2019;**22**(2):56–9.
27. Domnanich KA, Müller C, Benešová M *et al.* ^{47}Sc as useful β--emitter for the radiotheragnostic paradigm: a comparative study of feasible production routes. *EJNMMI Radiopharm Chem* 2017;**2**(1):5. https://doi.org/10.1186/s41181-017-0024-x.
28. Meulen NP Van der, Bunka M, Domnanich KA *et al.* Cyclotron production of ^{44}Sc: From bench to bedside. *Nucl Med Biol* 2015;**42**(9):745–51. https://doi.org/10.1016/j.nucmedbio.2015.05.005.
29. Gizawy MA, Mohamed NMA, Aydia MI *et al.* Feasibility study on production of Sc-47 from neutron irradiated Ca target for cancer theranostics applications. *Radiochim Acta* 2020;**108**(3):207–15. https://doi.org/10.1515/ract-2018-3070.
30. Filosofov D V., Loktionova NS, Rösch F. A ^{44}Ti/^{44}Sc radionuclide generator for potential application of ^{44}Sc-based PET-radiopharmaceuticals. *Radiochim Acta* 2010;**98**(3). https://doi.org/10.1524/ract.2010.1701.
31. Pruszyński M, Loktionova NS, Filosofov DV *et al.* Post-elution processing of ^{44}Ti/^{44}Sc generator-derived ^{44}Sc for clinical application. *Appl Radiat Isot* 2010;**68**(9):1636–41. https://doi.org/10.1016/j.apradiso.2010.04.003.
32. Schmidt CE, Groveman S, Sanders VA *et al.* Development of a SnO_2-based ^{44}Ti/^{44}Sc generator for medical applications. *J Chromatogr A* 2024;**1732**:465245. https://doi.org/10.1016/j.chroma.2024.465245.
33. Larenkov AA, Makichyan AG, Iatsenko VN. Separation of ^{44}Sc from ^{44}Ti in the Context of A Generator System for Radiopharmaceutical Purposes with the Example of [^{44}Sc]Sc-PSMA-617 and [^{44}Sc]Sc-PSMA-I&T Synthesis. *Molecules* 2021;**26**(21):6371. https://doi.org/10.3390/molecules26216371.
34. Miroshin P.A., Larenkov A.A. Cation exchange conditioning of the ^{44}Ti/^{44}Sc generator eluate for the production of scandium-44 solutions and synthesis of radiopharmaceuticals based on them. *Sorbtsionnye i Khromatograficheskie Protsessy* 2025;**25**(1):35–44. https://doi.org/10.17308/sorpchrom.2025.25/12792.
35. Reubi JC, Schär JC, Waser B *et al.* Affinity profiles for human somatostatin receptor subtypes SST1-SST5 of somatostatin radiotracers selected for scintigraphic and

radiotherapeutic use. *Eur J Nucl Med Mol Imaging* 2000;**27**(3):273–82. https://doi.org/10.1007/s002590050034.
36. Benešová M, Schäfer M, Bauder-Wüst U *et al.* Preclinical Evaluation of a Tailor-Made DOTA-Conjugated PSMA Inhibitor with Optimized Linker Moiety for Imaging and Endoradiotherapy of Prostate Cancer. *J Nucl Med* 2015;**56**(6):914–20. https://doi.org/10.2967/jnumed.114.147413.
37. Baum RP, Schuchardt C, Singh A *et al.* Feasibility, Biodistribution, and Preliminary Dosimetry in Peptide-Targeted Radionuclide Therapy of Diverse Adenocarcinomas Using ^{177}Lu-FAP-2286: First-in-Humans Results. *J Nucl Med* 2022;**63**(3):415–23. https://doi.org/10.2967/jnumed.120.259192.
38. Zboralski D, Hoehne A, Bredenbeck A *et al.* Preclinical evaluation of FAP-2286 for fibroblast activation protein targeted radionuclide imaging and therapy. *Eur J Nucl Med Mol Imaging* 2022;**49**(11):3651–67. https://doi.org/10.1007/s00259-022-05842-5.
39. Marhol M. *Ion Exchangers in Analytical Chemistry. Their Properties and Use in Inorganic Chemistry*. In: *Elsevier*, vol. 14. Prague, Czech Republic, 1982.
40. Coenen HH, Gee AD, Adam M *et al.* Consensus nomenclature rules for radiopharmaceutical chemistry — Setting the record straight. *Nucl Med Biol* 2017;**55**:v–xi. https://doi.org/10.1016/j.nucmedbio.2017.09.004.
41. Walczak R, Krajewski S, Szkliniarz K *et al.* Cyclotron production of ^{43}Sc for PET imaging. *EJNMMI Phys* 2015;**2**(1):33. https://doi.org/10.1186/s40658-015-0136-x.
42. Müller C, Bunka M, Reber J *et al.* Promises of Cyclotron-Produced ^{44}Sc as a Diagnostic Match for Trivalent β^- -Emitters: In Vitro and In Vivo Study of a ^{44}Sc-DOTA-Folate Conjugate. *J Nucl Med* 2013;**54**(12):2168–74. https://doi.org/10.2967/jnumed.113.123810.
43. Gallium (^{68}Ga) chloride solution for radiolabelling, Monograph 2464. Ph. Eur. Supp. 12.1. Strasbourg, France: Council of Europe; 2026. n.d. https://pheur-online.edqm.eu/home/.
44. Bharate SS. Carboxylic Acid Counterions in FDA-Approved Pharmaceutical Salts. *Pharm Res* 2021;**38**(8):1307–26. https://doi.org/10.1007/s11095-021-03080-2.
45. Huclier-Markai S, Medvedev DG, Cutler CS. Improved titanium-44 purification process for establishing a high apparent molar activity titanium-44/scandium-44 generator. *Appl Radiat Isot* 2024;**212**:111451. https://doi.org/10.1016/j.apradiso.2024.111451.
46. Shannon R. Revised Effective Ionic Radii and Systematic Studies of Interatomic Distances in Halides and Chalcogenides. *Acta Cryst* 1976;**32**:751–67.
47. Pniok M, Kubíček V, Havlíčková J *et al.* Thermodynamic and Kinetic Study of Scandium(III) Complexes of DTPA and DOTA: A Step Toward Scandium Radiopharmaceuticals. *Chem – A Eur J* 2014;**20**(26):7944–55. https://doi.org/10.1002/chem.201402041.
48. Horovitz CT. Interactions of Scandium and Yttrium with Molecules of Biological Interest. In: *Biochemistry of Scandium and Yttrium, Part 1: Physical and Chemical Fundamentals*. Boston, MA: Springer US, 1999, 235–308. https://doi.org/10.1007/978-1-4615-4313-8_6.
49. Itoh H, Itoh N, Suzuki Y. Stability Constants of Scandium Complexes. I. Monocarboxylate Complexes Species. *Bull Chem Soc Jpn* 1984;**57**(3):716–8. https://doi.org/10.1246/bcsj.57.716.
50. Skorik NA, Artish AS. The stability of the complexes of scandium, gallium, indium, and thorium with the anions of various organic acids. *Russ J Inorg Chem* 1985;**30**:1130–2.
51. Itoh H, Ikegami Y, Suzuki Y. Stability Constants of Scandium Complexes. II. Dicarboxylate Complexes Species. *Bull Chem Soc Jpn* 1984;**57**(12):3426–9. https://doi.org/10.1246/bcsj.57.3426.
52. International Council for harmonisation. *ICH Q3C(R8) Impurities: Guideline for Residual-Solvents.* Geneva, 2021. https://www.ich.org/page/q3c-residual-solvents.

Figure legends

Fig. 1. ^{44}Sc distribution coefficient (mean ± SD, mL/g; n = 5) in 0.1 M HCl, in 1 M sodium acetate (pH 4.00 ± 0.15) and in the undiluted generator eluate (0.1 M $H_2C_2O_4$/0.2 M HCl) for the cation-exchange resins examined. Batch method; V = 1 mL, m = 15.0 mg, 24 h at 20 °C. The value for OASIS MCX CC in 0.1 M HCl exceeds the limit of quantification of the method (the grey-shaded region above 6.6 × 10^3 mL/g, Eq. 2) and is shown as censored.

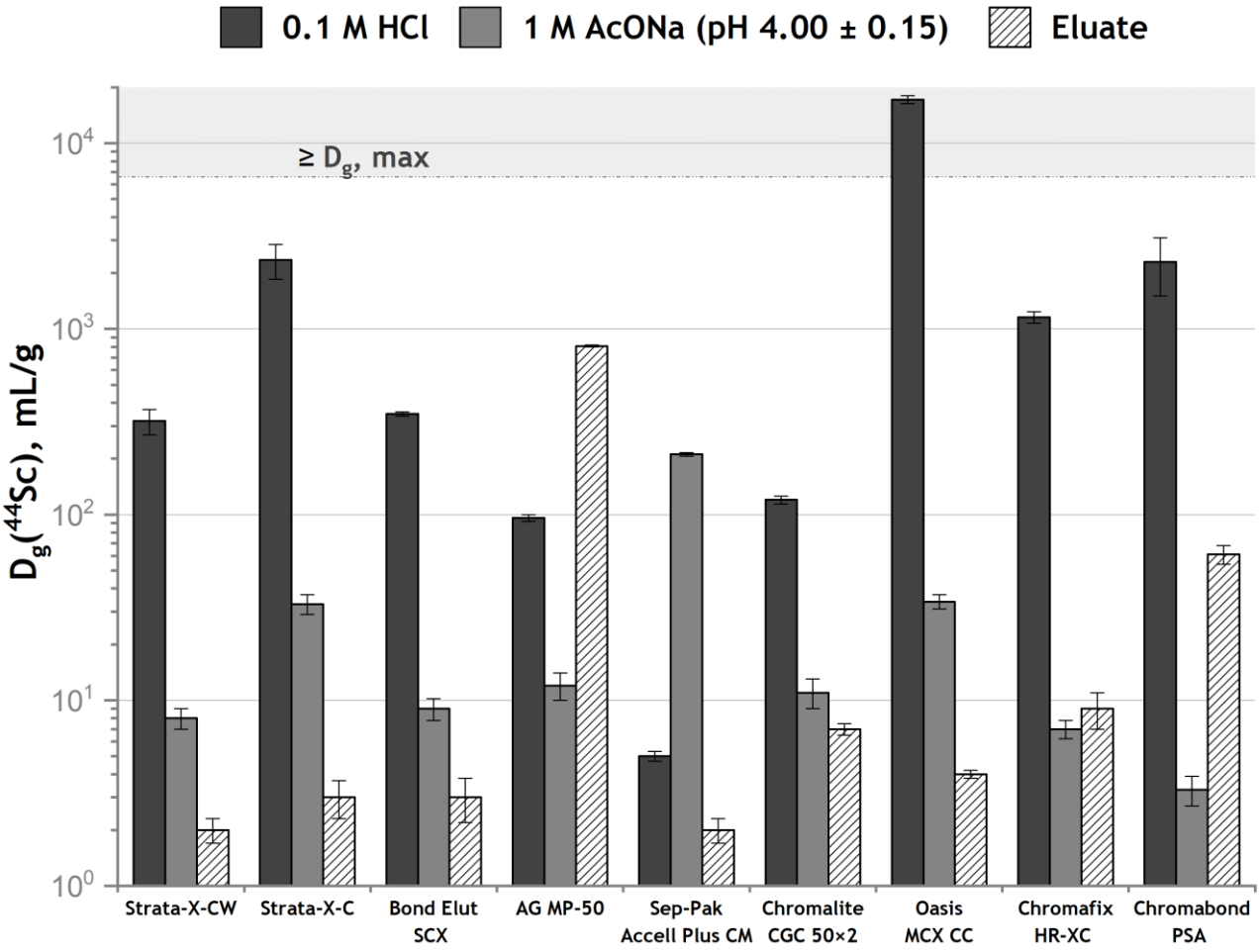


Fig. 2. Distribution coefficient of ^{44}Sc (mean ± SD, mL/g; n = 5) as a function of the dilution factor of the generator eluate for (A) Chromafix HR-XC and (B) Chromabond PSA. Dilution factor = V(final)/V(eluate); the undiluted eluate corresponds to a factor of 1. Red dashed line: 0.1 M HCl (pink area: mean ± SD). The grey-shaded region above 6.6 × 10^3 mL/g lies beyond the limit of quantification of the batch method at V/m = 66.7 mL/g (Eq. 2).

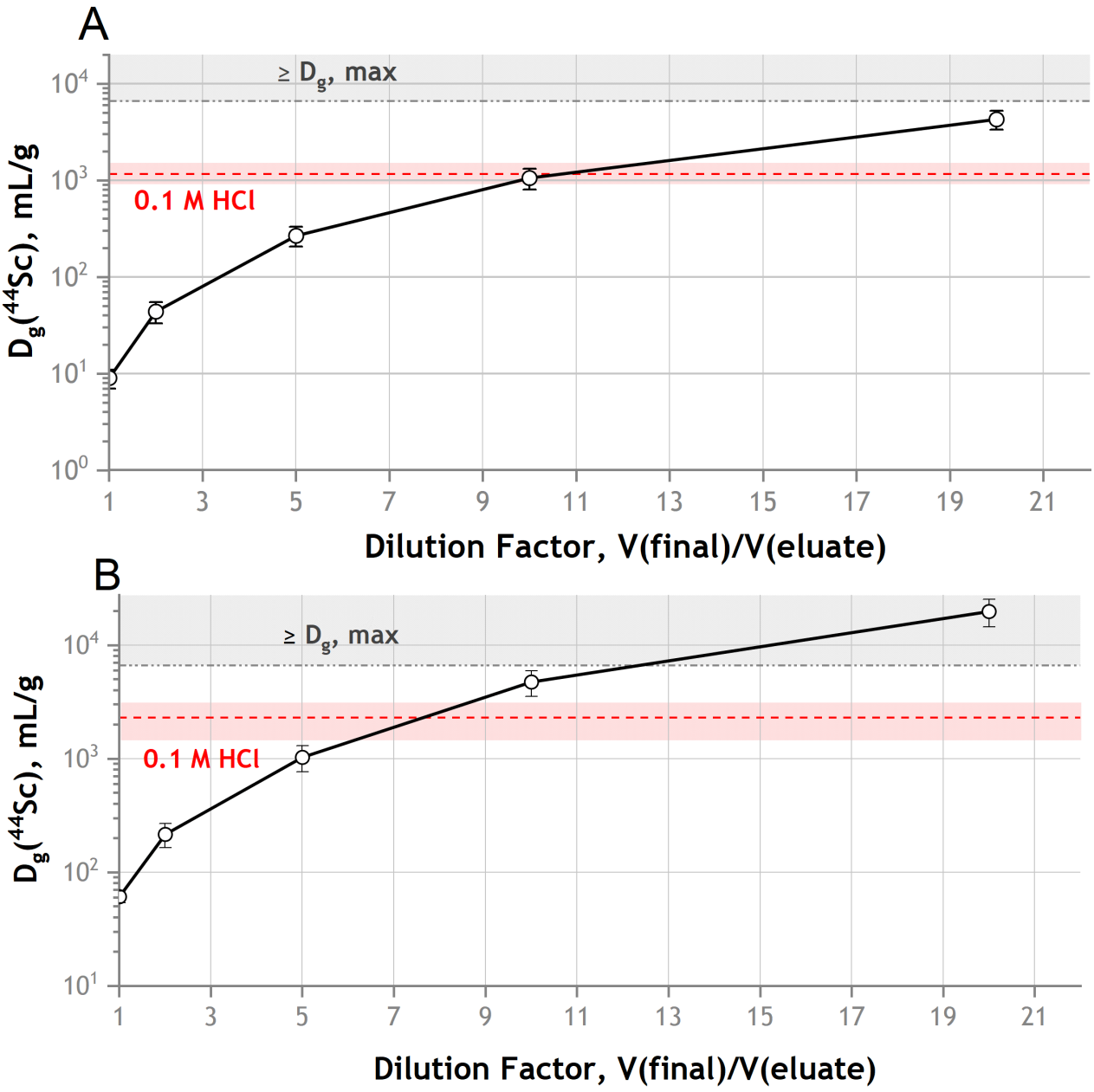


Fig. 3. Sorption of ^{44}Sc (decay-corrected; mean ± SD, %; n = 5) from 0.1 M HCl, from the generator eluate (0.1 M $H_2C_2O_4$/0.2 M HCl) and from fivefold diluted eluate (0.02 M $H_2C_2O_4$/0.04 M HCl) on the cation-exchange resins examined. Percentages refer to the activity applied to the column; resin masses are given in Table 4.

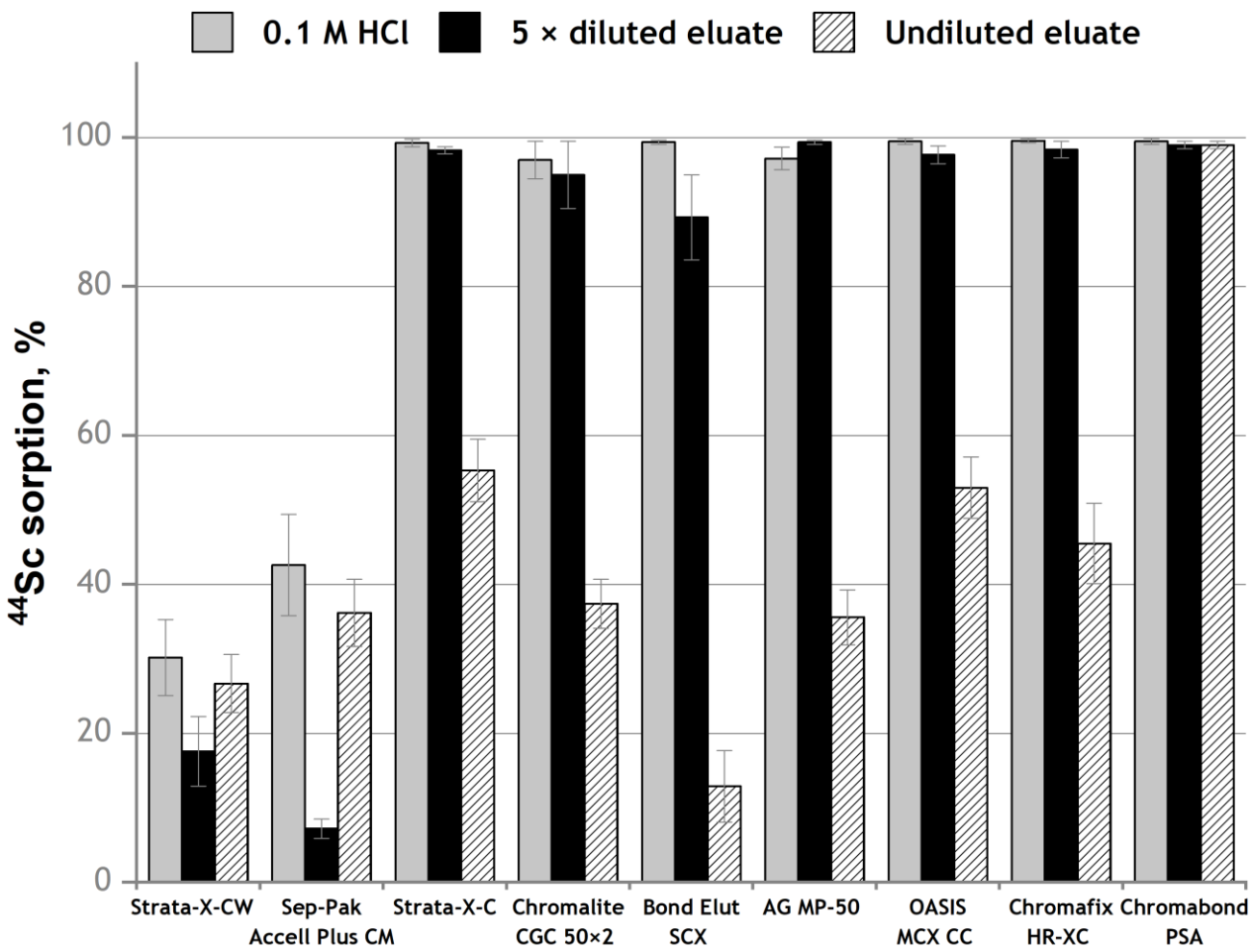


Fig. 4. Sorption of ^{44}Sc (decay-corrected; mean ± SD, %; n = 5) on Chromafix HR-XC as a function of the dilution factor of the generator eluate.

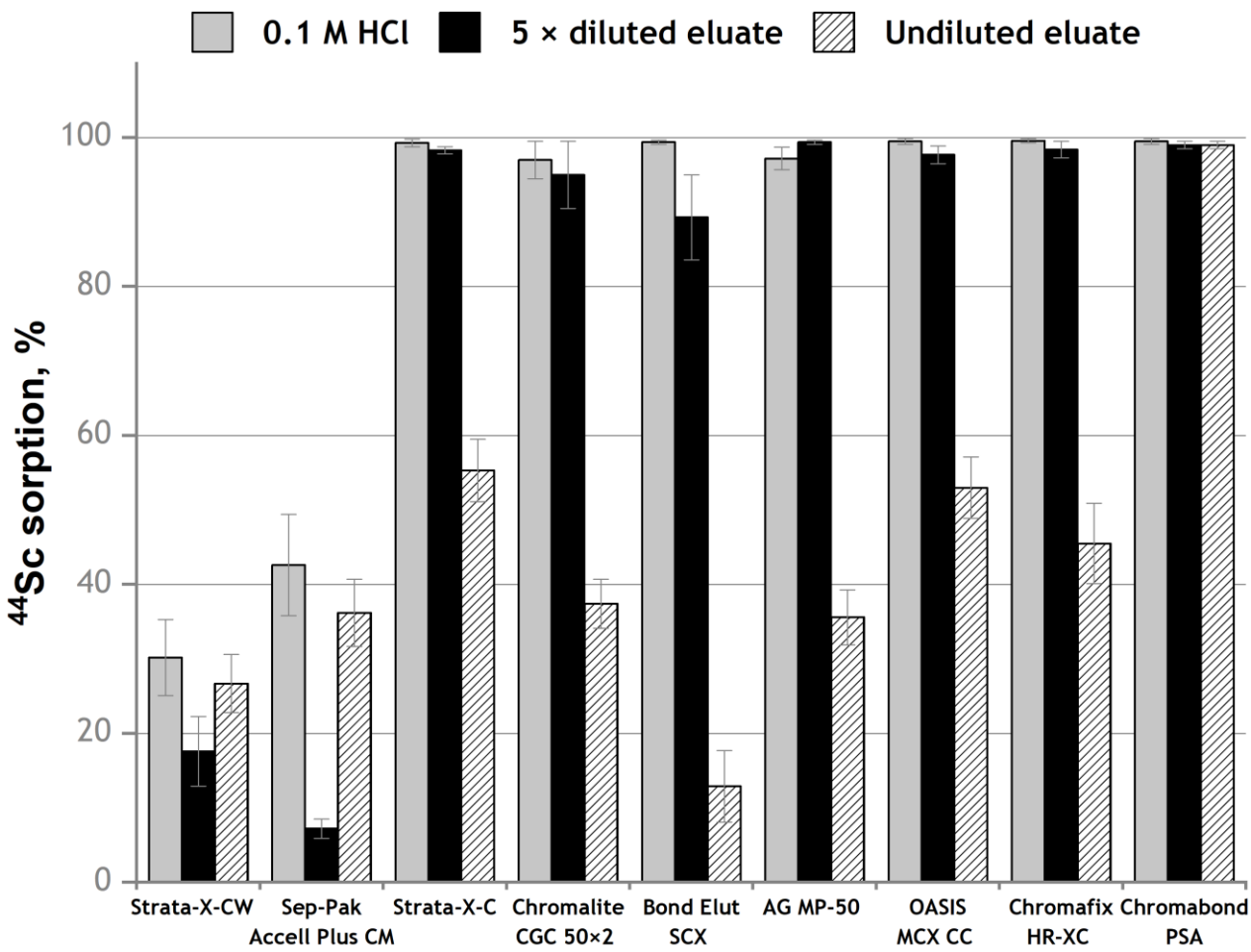


Fig. 5. Sorption of ^{44}Sc (decay-corrected; mean ± SD, %; n = 5) from the undiluted eluate as a function of the mass of Chromabond PSA in the column. All points were obtained on 100 × 2.1 mm columns.

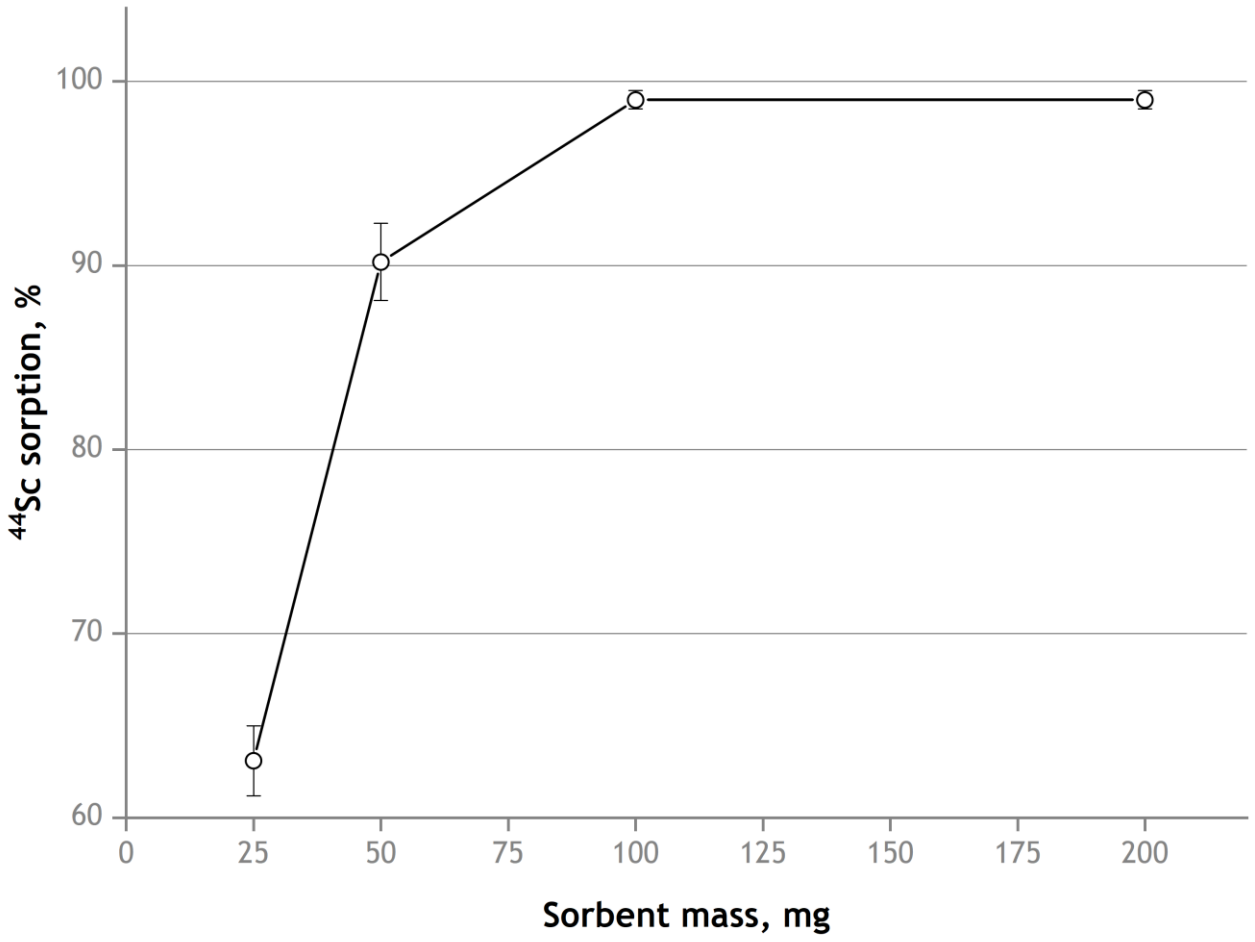


Fig. 6. Distribution coefficient of ^{44}Sc (mean ± SD, mL/g; n = 5) for Chromafix HR-XC and Chromabond PSA (A) as a function of sodium acetate concentration at pH 4.00 ± 0.15 and (B) as a function of pH in 1 M sodium acetate.

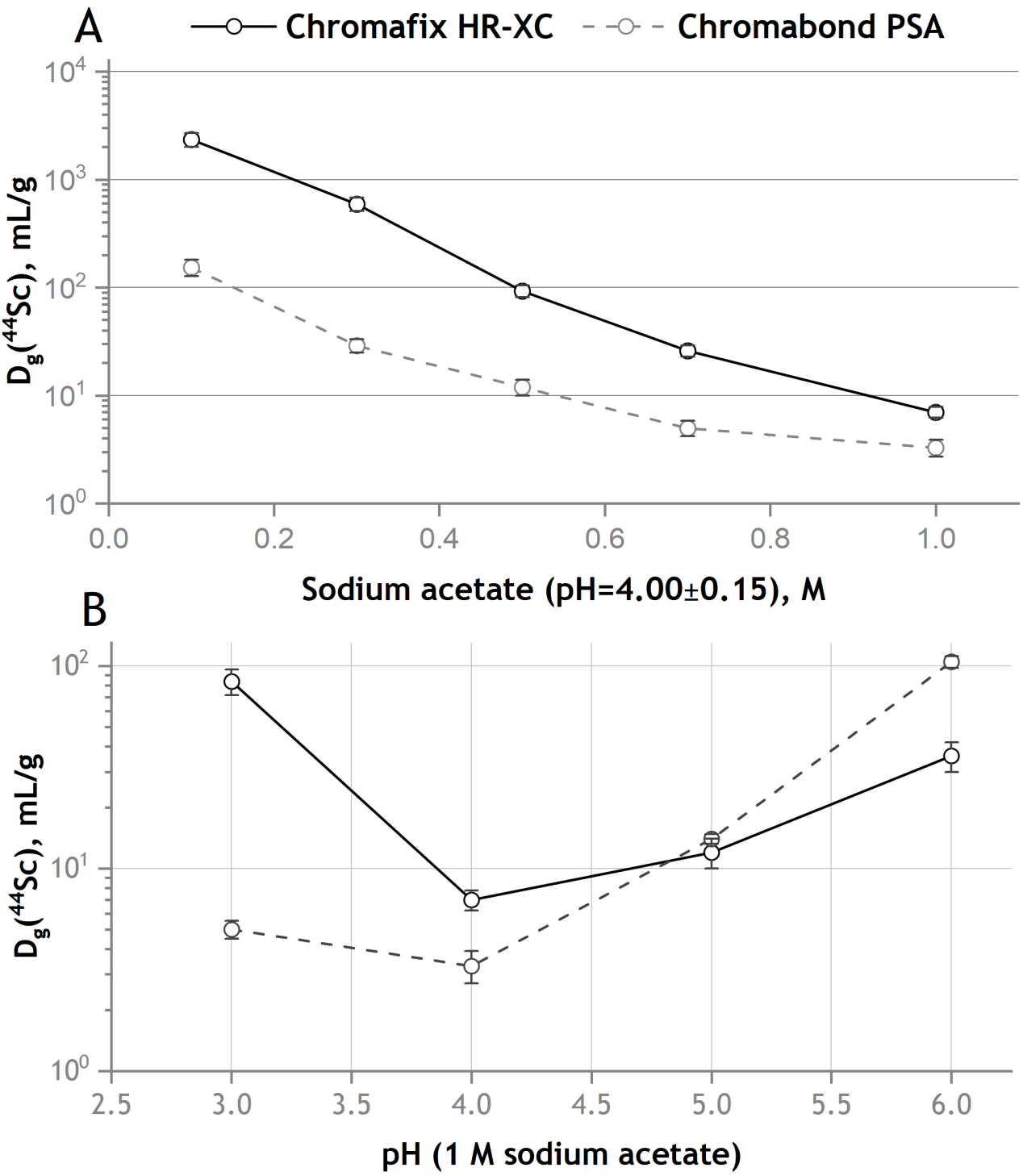


Fig. 7. Recovery of ^{44}Sc (decay-corrected; mean ± SD, %; n = 5) in 1 mL of 1 M sodium acetate (pH 4.00 ± 0.15) from the cation-exchange resins examined. Hatched bars denote the four resins carried forward to the labelling experiments; the dashed line at 70% is drawn for reference only.

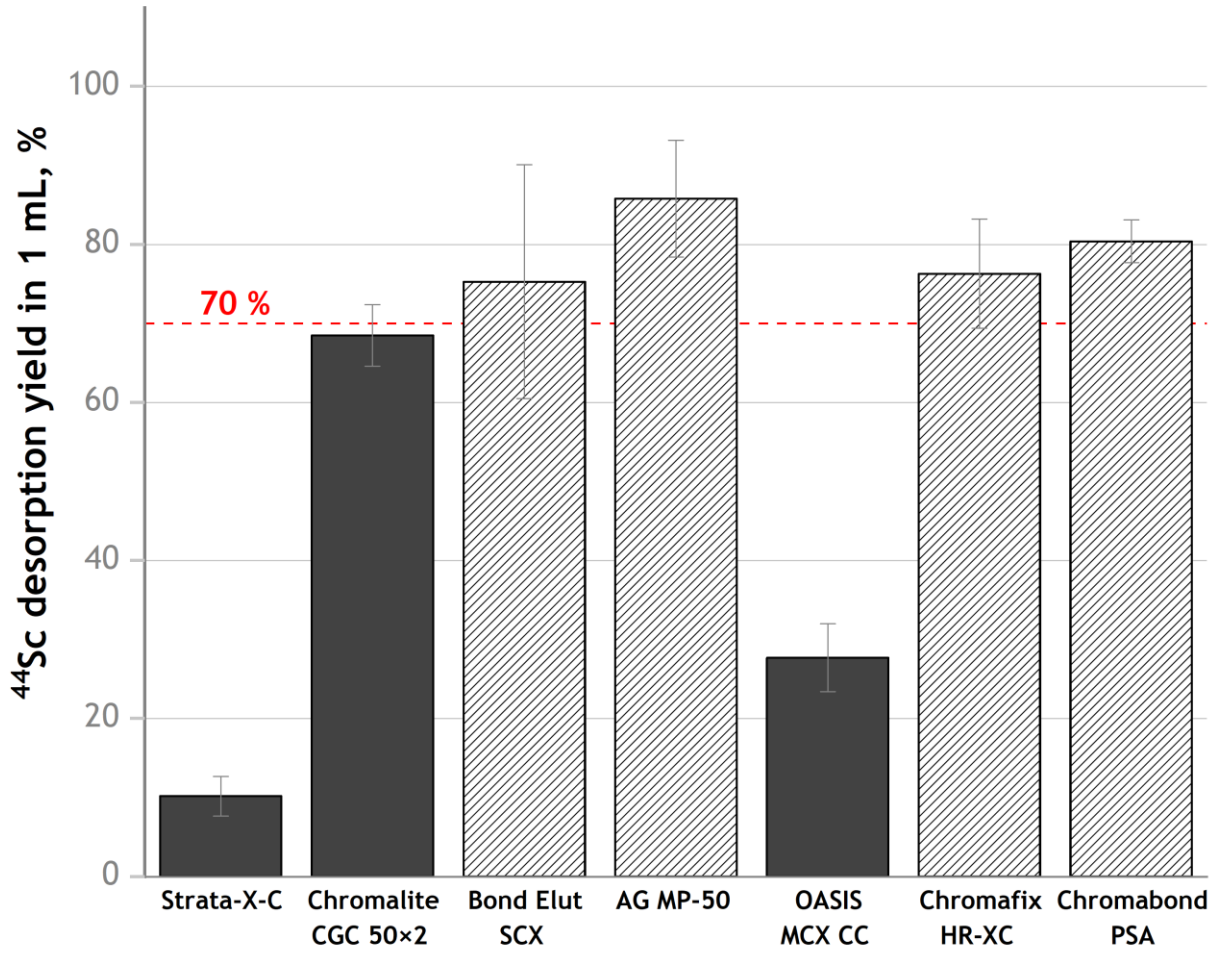


Fig. 8. Elution profiles of ^{44}Sc with 1 M sodium acetate (pH 4.00 ± 0.15), 0.5 mL fractions: (A) AG MP-50, (B) Bond Elut SCX, (C) Chromafix HR-XC, (D) Chromabond PSA. Ordinate: per-fraction recovery as a percentage of the activity applied. Cumulative recoveries over the first 1 mL are 85.7 ± 11.5, 74.4 ± 15.2, 74.2 ± 8.7, and 80.5 ± 7.2 %.

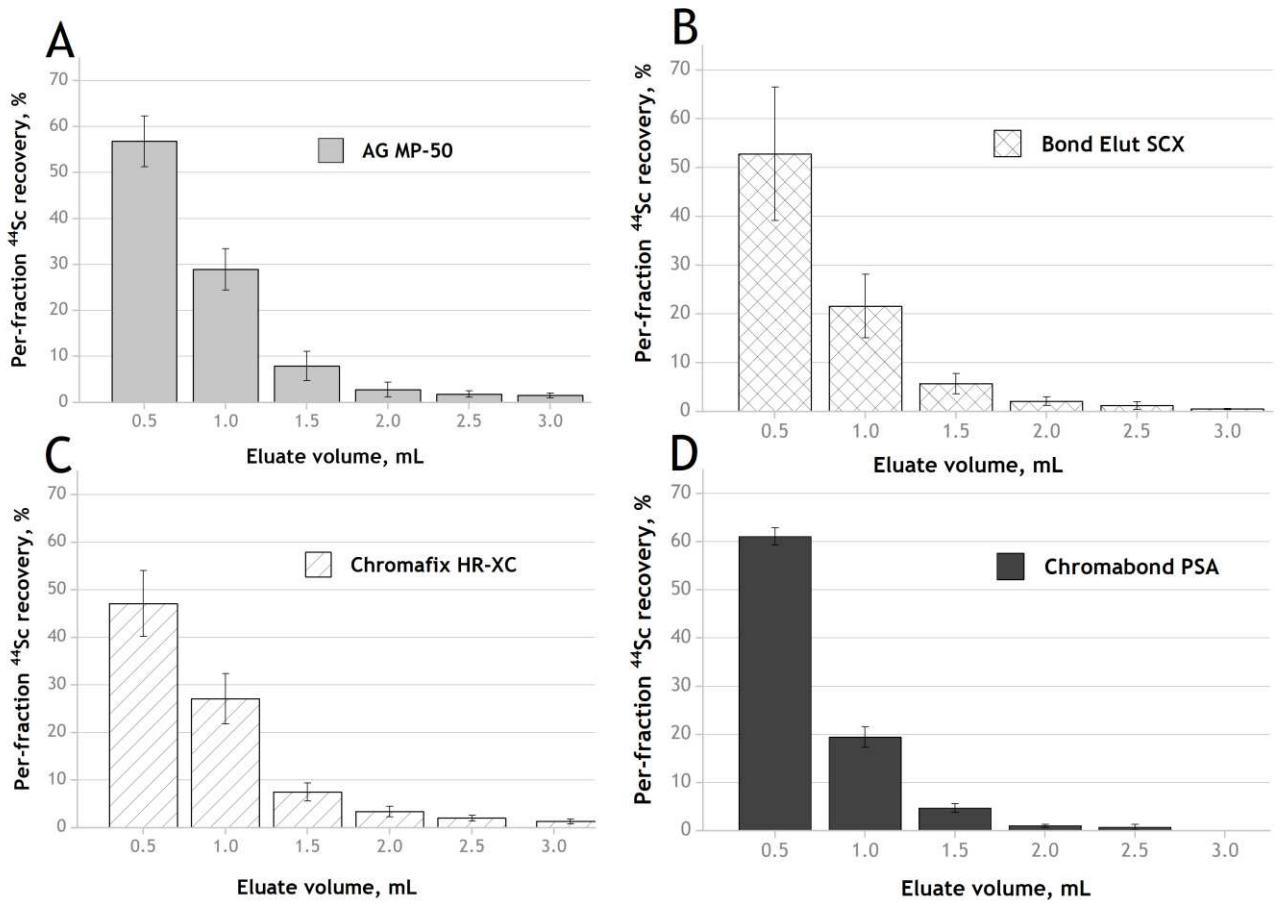


Fig. 9. Radiochemical yield of [^{44}Sc]Sc-PSMA-617 (mean ± SD, %; n = 5) versus reaction time for ^{44}Sc eluates from the four selected resins. Conditions: 95 °C, V = 1.0 mL, 1 M sodium acetate (pH 4.00 ± 0.15), V_p = 5 µL (4.78 nmol) precursor. The dashed line at 95 % is drawn for reference only. This kinetic comparison was performed at V_p = 5 µL (4.78 nmol); the preparations summarized in Table 6 were made separately at V_p = 1 µL.

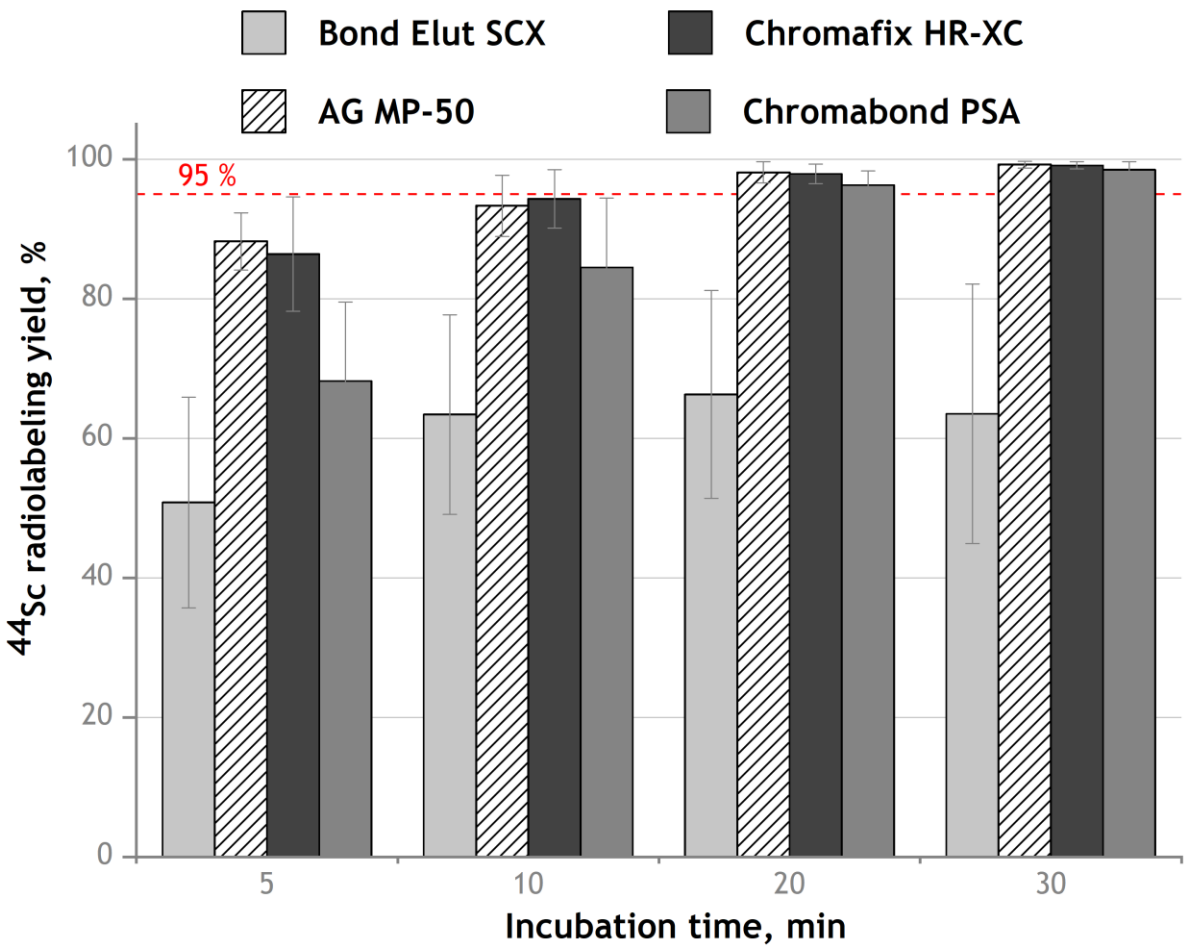


Fig. 10. Recovery of ^{44}Sc (decay-corrected; mean ± SD, %; n = 5) from Chromafix HR-XC with six carboxylate eluents at 0.2–1.0 M (1 mL, pH 4.00 ± 0.15).

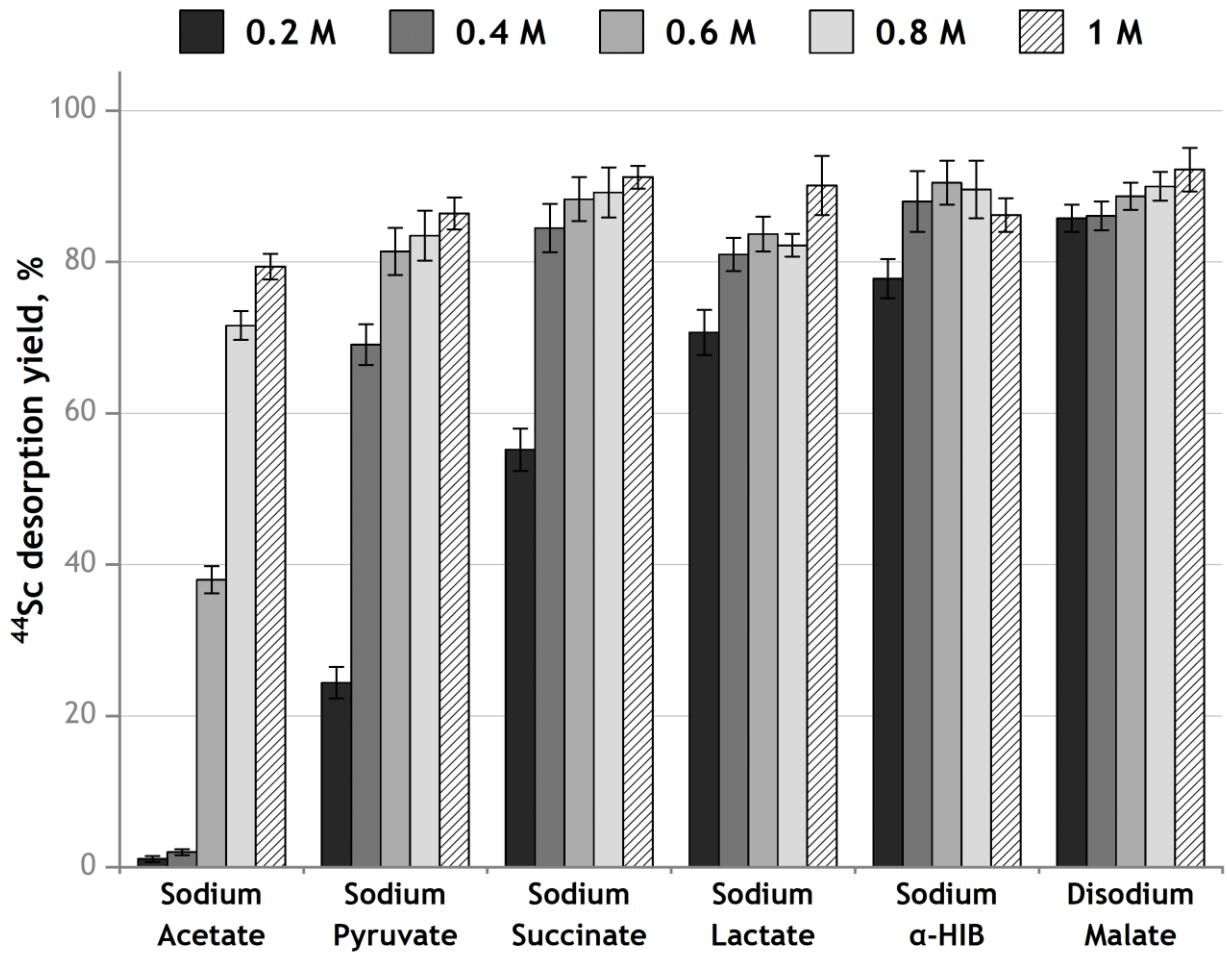


Fig. 11. Radiochemical yield of [^{44}Sc]Sc-DOTA-TATE (mean ± SD, %; n = 5) in the same six carboxylate media at 0.2–1.0 M. Conditions: 95 °C, V = 1.0 mL, pH 4.00 ± 0.15. The V_p = 20 µL (13.9 nmol) precursor amount was chosen for screening; the selected eluent was subsequently validated at V_p = 1 µL (0.7 nmol).

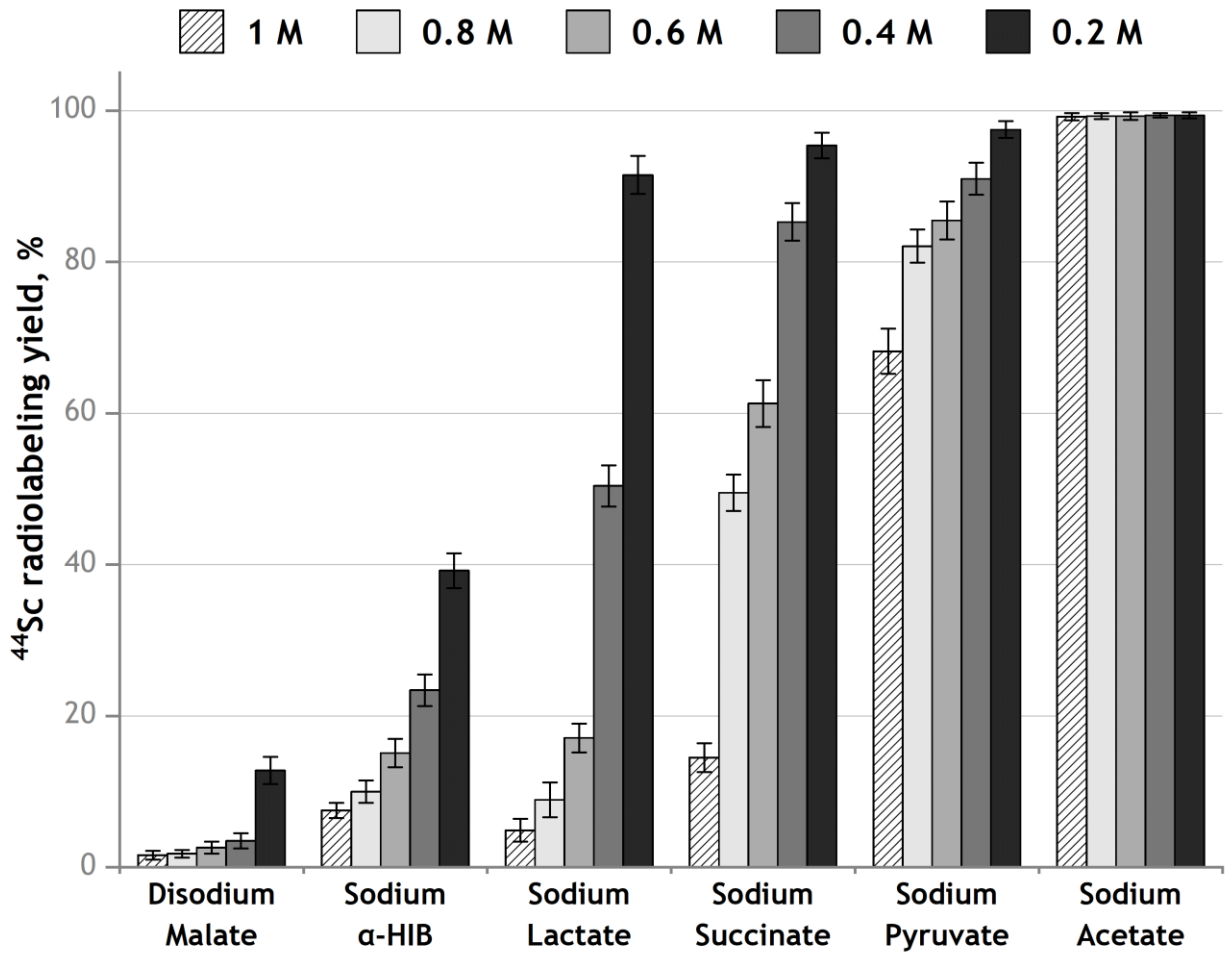


Fig. 12. Combined criterion $Y_{comb} = Y_{des} \times RCY$ for the six carboxylate eluents at five concentrations, computed from the data of Figs. 10 and 11. The global maximum is 1 M sodium acetate.'

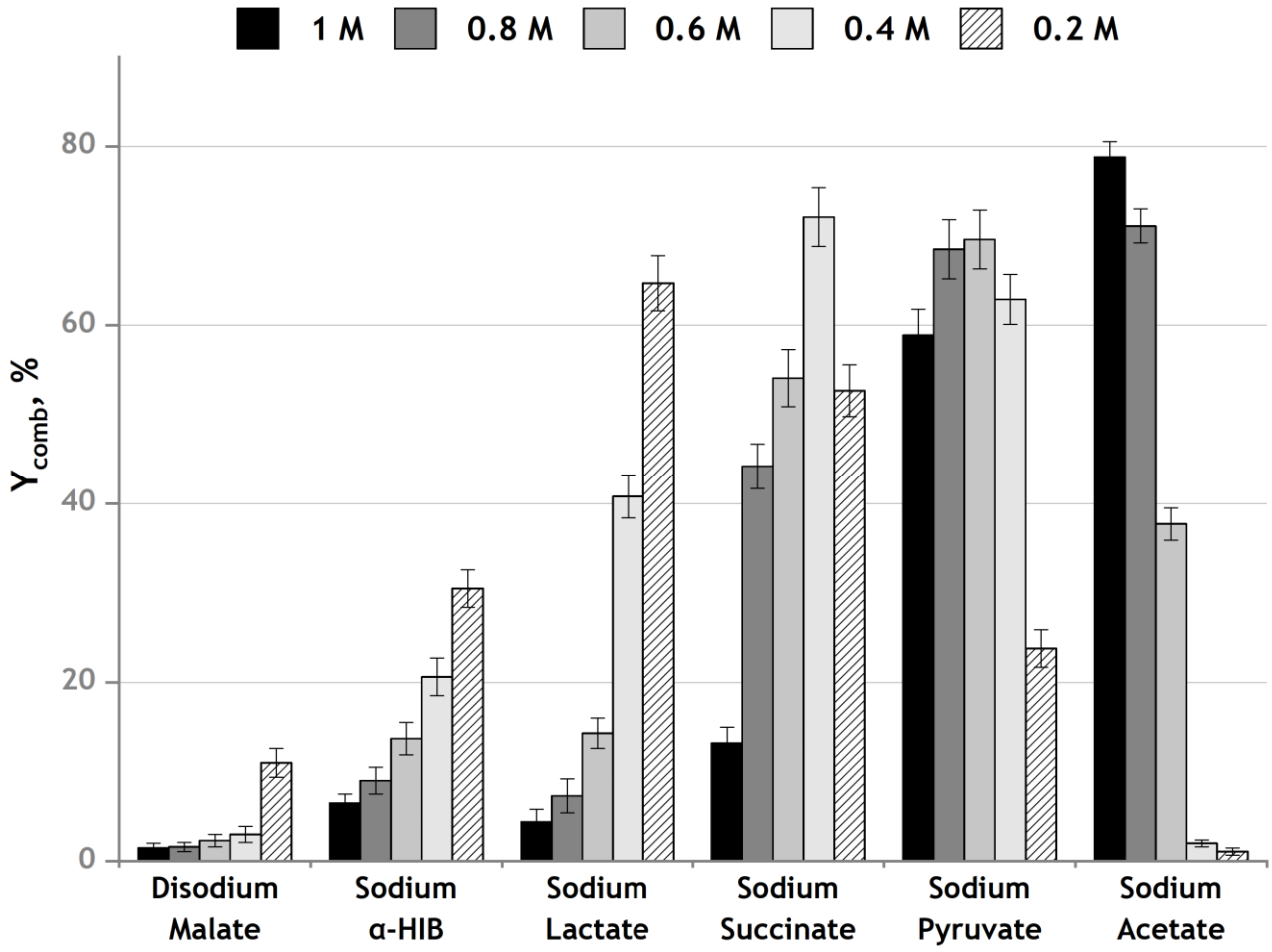
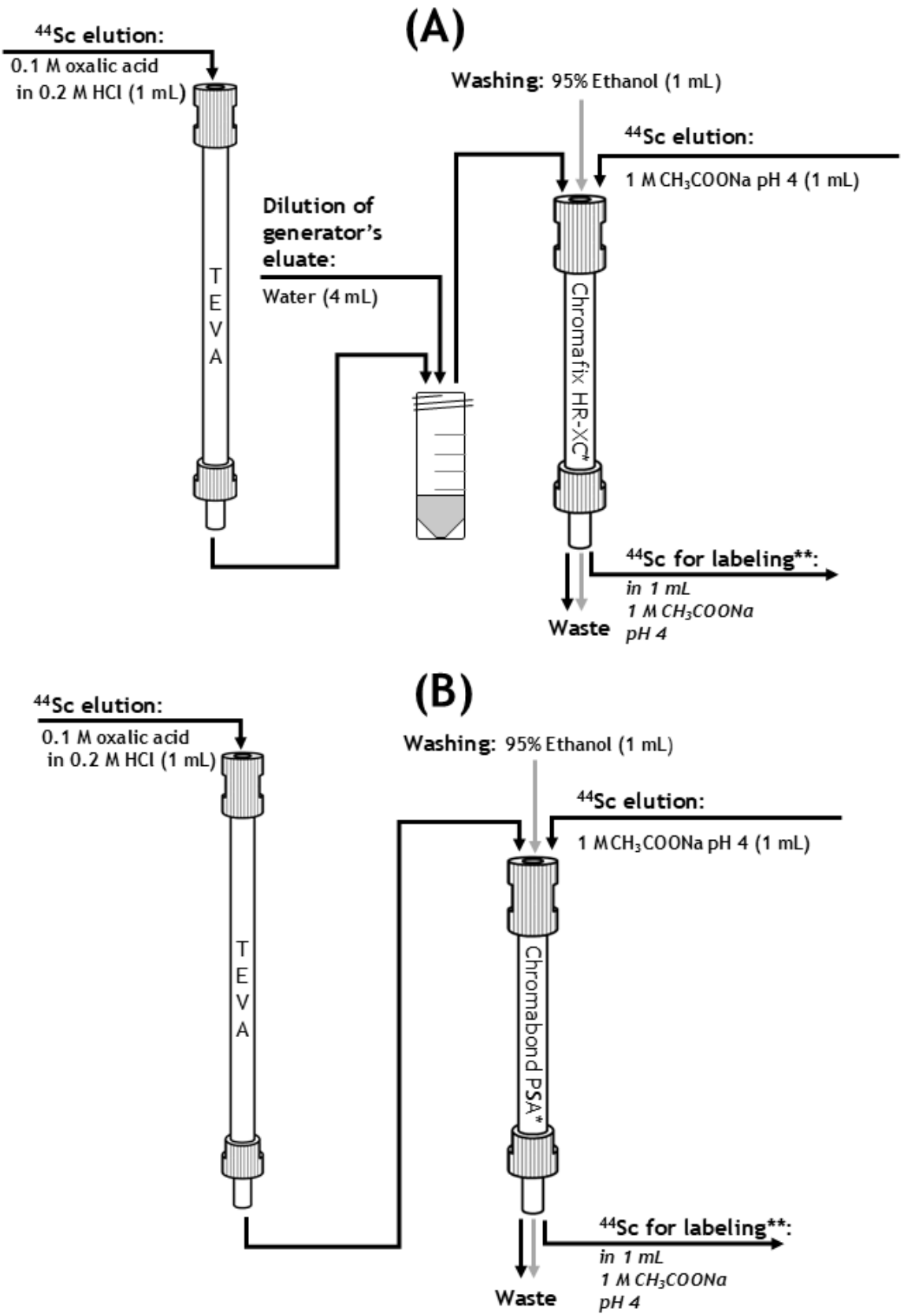


Fig. 13. Post-elution processing schemes for the TEVA-based $^{44}Ti/^{44}Sc$ generator eluate based on (A) Chromafix HR-XC and (B) Chromabond PSA. Resin masses (mg), total process times (min) and flow rates (*f*, mL/min) are indicated.



**Loaded mass; **Total process time:*

(A) — *63 mg; 15 min*

(B) — *100 mg; 11 min*

***f* = 1 mL/min**

Supplementary Files

This is a list of supplementary files associated with this preprint. Click to download.

- Supplementaryinformation.docx